

# Gravitational waves from patterns of electroweak symmetry breaking: an effective perspective

Rong-Gen Cai,<sup>1,2,3,4,5,\*</sup> Katsuya Hashino,<sup>6,7,†</sup> Shao-Jiang Wang,<sup>2,8,‡</sup> and Jiang-Hao Yu<sup>2,3,4,5,§</sup>

<sup>1</sup>*Institute of Fundamental Physics and Quantum Technology, Ningbo University, Ningbo, 315211, China*

<sup>2</sup>*CAS Key Laboratory of Theoretical Physics, Institute of Theoretical Physics, Chinese Academy of Sciences, Beijing 100190, China*

<sup>3</sup>*School of Physical Sciences, University of Chinese Academy of Sciences (UCAS), Beijing 100049, China*

<sup>4</sup>*School of Fundamental Physics and Mathematical Sciences, Hangzhou Institute for Advanced Study (HIAS), University of Chinese Academy of Sciences, Hangzhou 310024, China*

<sup>5</sup>*International Centre for Theoretical Physics Asia-Pacific, Beijing/Hangzhou, China*

<sup>6</sup>*Center for High Energy Physics, Peking University, Beijing 100871, China*

<sup>7</sup>*National Institute of Technology, Fukushima College, Nagao 30, Taira-Kamiarakawa, Iwaki, Fukushima 970-8034, Japan*

<sup>8</sup>*Asia Pacific Center for Theoretical Physics (APCTP), Pohang 37673, Korea*

The future space-borne gravitational wave (GW) detectors would provide a promising probe for the new physics beyond the standard model that admits the first-order phase transitions. The predictions for the GW background vary sensitively among different concrete particle physics models but also share a large degeneracy in the model buildings, which motivates an effective model description on the phase transition based on different patterns of the electroweak symmetry breaking (EWSB). In this paper, using the scalar  $N$ -plet model as a demonstration, we propose an effective classification for three different patterns of EWSB: (1) radiative symmetry breaking with classical scale invariance, (2) Higgs mechanism in generic scalar extension, and (3) higher dimensional operators. We conclude that a strong first-order phase transition could be realized for (1) and (2) with a small quartic coupling and a small isospin of an additional  $N$ -plet field for the light scalar field model with and without the classical scale invariance, and (3) with a large mixing coupling between scalar fields and a large isospin of the  $N$ -plet field for the heavy scalar field model.

## I. INTRODUCTION

Despite of the success of the standard model (SM) of particle physics [1] as a low-energy effective field theory (EFT), it is incomplete in describing the puzzles of dark energy, dark matter (DM), cosmic inflation and baryon asymmetry of our Universe (BAU). The proposed solutions might call for a larger symmetry group for the ultraviolet (UV) completion, which should be broken into the SM symmetry group in our current epoch. Some of these symmetry breakings would trigger cosmic first-order phase transitions (FOPTs) (see [2] for a comprehensive review and [3] for a pedagogical lecture) proceeding by the bubble nucleations, bubble expansion and bubble collisions, which would generate a stochastic background of gravitational waves (GWs) (see [4, 5] for recent reviews from LISA Collaboration [6] and [7, 8] for earlier reviews from eLISA/NGO mission [9]; see also [10] for a brief review) transparent to our early Universe that is otherwise opaque to light for us to probe via electromagnetic waves if the FOPTs occurs before the recombination epoch. Therefore, the GWs detection serves as a promising and unique probe [11, 12] for the new physics [13, 14] beyond SM (BSM) with FOPTs.

Since the SM admits no FOPT but a cross-over transition due to a relatively heavy Higgs mass [15], any model buildings with FOPTs should go beyond SM. However, a clean separation for BSM new physics with FOPTs from those without FOPTs turns out to be difficult, so does a clear classification for various FOPT models. Usually the FOPT models could be naively classified into models extended with higher-dimensional operators [16–39], scalar singlet [40–73]/doublet [74–91]/triplet [92–104]/quadruplet [30], composite Higgs [18, 19, 105–117], supersymmetry (SUSY) [118–144], warp extra-dimensions [116, 117, 145–184], and dark/hidden sectors [113, 164, 171, 185–242], which, however, are actually overlapping with each other when focusing on the sector that actually induces a FOPT. Nevertheless, most of the FOPT models could be regarded effectively as some kind of scalar extensions of the SM, while other FOPT models with fermion extensions [243–247] are special on their own for triggering a PT, we therefore only focus on the scalar extensions of the SM.

On the other hand, some of the scalar extensions of the SM could be described and parametrized in the effective field theory (EFT) framework, in which the new particles are integrated out and only the SM degrees of freedom are kept. The EFT description was adopted before particularly for the higher-dimensional-operator extensions of the SM, which characterize the effect on the low-energy degrees of freedom when we integrate out the heavy degrees of freedom. However, the EFT description is only valid in the presence of a clear separation of

\* cairg@itp.ac.cn

† hashino@fukushima-nct.ac.jp

‡ schwang@itp.ac.cn

§ jhyu@itp.ac.cn

scales, which is in conflict with the relatively low scale of the new degrees of freedom so as to introduce a large correction to the SM Higgs potential [248] in order to trigger a PT. Exceptions could be made for the Higgs-singlet extension with tree-level matching, though the EFT description is at most qualitative for dimension-six extension. Recently, a new perspective on this SM EFT description is made if the potential barrier separating the two minimums is generated radiatively instead of the tree-level barrier [249]. Nevertheless, we have found in this paper that the difficulty of an EFT description for the FOPT models could be circumvented by introducing a large number of scalar fields in the  $N$ -plet scalar field model. Therefore, for the electroweak phase transition process, the EFT description for some scalar extensions is not enough since in many cases the new light degree of freedom would contribute to the thermal plasma and thus one cannot integrate it out during phase transition. See also [250–252] for the dimensionally reduced effective field theory and its applications on reducing the uncertainties from the renormalisation scale dependence [253, 254] and the thermal bubble nucleation calculation [255–257].

In this paper we instead take an intermediate strategy that lays between the specific new physics model and EFT treatment. We utilize a simplified model to illustrate feature of the electroweak phase transition (EWPT), which we call the effective model description on the phase transition. In this description, to capture different patterns of the EWPT and to compare the difference between new physics model and EFT description, we propose a specific effective model description: the general model extends the SM with an isospin  $N$ -plet scalar field, of which the light scalar case consists of a model with classical scale invariance (CSI) (model I) and a model without CSI (model II), while the heavy scalar case is simply a model with higher-dimensional operators, for example, a dimension-six operator (model III). The above cases could describe the patterns of the electroweak symmetry breaking (EWSB) via, for example, (1) radiative symmetry breaking, (2) Higgs mechanism, and (3) EFT description of EWSB. Our effective model description already covers those scalar models with  $N$ -plet on the market, such as (1) singlet models including a real scalar singlet extension of SM (xSM), composite Higgs model like SO(6)/SO(5) model, extra dimension model like radion model, dilaton model; (2) doublet models including SUSY model like minimal supersymmetry model (MSSM), two Higgs doublet model (2HDM), minimal dark matter model; (3) triplet models including left-right model, Type-II seesaw model. In other perspective, our effective model description consists of the simplified models (effective models I and II) for the realistic models (SUSY, composite Higgs, etc.) and an EFT model (model III). Therefore, our effective model provide an effective description for the EWSB that could admit a FOPT with associated GWs.

Although the effective scalar models describe different

EWSB patterns, they share the same form of the Higgs potential. Thus, utilizing the polynomial potential form, we could analyse how the FOPT is realized in different cases. To show the source of a sizable barrier for realizing the first-order EWPT, we consider the following polynomial potential form in each of three models,

$$V_p = C_2\phi^2 + C_3\phi^3 + C_4\phi^4 + C_6\phi^6, \quad (1)$$

where  $\phi$  is the order parameter in the effective potential, and  $C_n$  are the effective couplings of  $\phi^n$ . The  $\phi^2$  and  $\phi^4$  term can appear in it at tree-level, on the other hand, the  $\phi^6$  term comes from high dimensional operator in the model (III). The  $\phi^3$  is the source of the first-order phase transition in the models (I) and (II), and it can be produced by the thermal loop effects. Let us summarize the main features and also the main results of this work on realizing the FOPT in the forementioned three models:

- For model I, there are no massive parameters, and we consider the EWPT along a flat direction in the tree-level potential to avoid invalidating the perturbative analysis, and thus the potential form with finite temperature effects are roughly given by  $V_p = C_2\phi^2 + C_3\phi^3 + C_4\phi^4$ , where all terms are one-loop level effects coming from thermal loop effects and radiative corrections.
- For model II, there are massive parameters in the Lagrangian unlike the model I. The potential of this model is still roughly given by  $V_p = C_2\phi^2 + C_3\phi^3 + C_4\phi^4$  but the tree-level effects are now in  $\phi^2$  and  $\phi^4$  terms.
- For model III, the high dimensional operator shows up in the potential  $V_p = C_2\phi^2 + C_3\phi^3 + C_4\phi^4 + C_6\phi^6$ , where the tree-level effects are in  $\phi^2$ ,  $\phi^4$  and  $\phi^6$  terms.

The main contributions to  $C_n\phi^n$  in each of these models are summarized in Tab. I. In the case of model I, not only  $C_3$  term but also  $C_2$  and  $C_4$  terms are from loop level effects, and then the strongly first-order EWPT can be easily realized. On the other hand, the model II receives tree-level effects from the  $C_2$  and  $C_4$  terms. The source of barrier for the models I and II is the negative  $C_3$  term from the thermal loop effects of bosons. The model III has the high dimensional operator  $C_6$ , and thus we can have a negative  $C_4$  term to generate a sizable barrier. That is different point from models I and II.

The outline of this paper is as follows: in section II we introduce our effective model description, whose effective potentials are detailed in section III. The resulted GWs from the FOPT models described above are extracted in a way depicted in section IV. The FOPT predictions are summarized in section V. The last section VI is devoted for conclusions and discussions. Appendix A is for some details on the model without CSI.

Model	$C_2\phi^2$	$C_3\phi^3$	$C_4\phi^4$	$C_6\phi^6$
I	Loop	Loop	Loop	None
II	Tree	Loop	Tree	None
III	Tree	Loop	Tree	Tree

TABLE I. The potential forms in the three types of the models where the EWSB occurs via (I) radiative symmetry breaking; (II) Higgs mechanism; (III) EFT description. Here,  $\phi$  is order parameter, and  $C_n$  is the effective coupling of  $\phi^n$ . The cubic term can be produced by thermal loop effects of bosons. To generate a sizable barrier, the cubic term will be negative in models I and II. In the model III, the quartic term can be negative to generate the barrier.

## II. EFFECTIVE MODELS

We focus on the model with an additional isospin  $N$ -plet scalar field  $\Phi_2 \sim (I_{\Phi_2}, Y_{\Phi_2})$  charged under  $SU(2)_I \times U(1)_Y$  gauge symmetry, where  $I_{\Phi_2}$  is the isospin and  $Y_{\Phi_2}$  is the hypercharge. The scalar boson fields in the model are given by

$$\Phi_1 = \begin{pmatrix} G^\pm \\ \frac{h+iG^0}{\sqrt{2}} \end{pmatrix}, \quad \Phi_2 = \frac{1}{\sqrt{2}} \begin{pmatrix} \phi_1 + i\phi_{1,i} \\ \phi_2 + i\phi_{2,i} \\ \vdots \\ \phi_N + i\phi_{N,i} \end{pmatrix}, \quad (2)$$

where  $\Phi_1$  is the SM-like double scalar field and  $\phi_n$  ( $\phi_{n,i}$ ) is the real (imaginary) part of the additional isospin  $N$ -plet scalar field with  $N \equiv 2I_{\Phi_2} + 1$ . These scalar bosons  $\Phi_1$ ,  $\Phi_2$  have classical fields:  $\langle \Phi_1 \rangle / \sqrt{2}$  and  $\langle \Phi_2 \rangle / \sqrt{2}$ , which are related to the real part of the neutral scalar field. We will discuss the testability from the GW detection for three types of the extended models instead on different patterns of the EWSB. These models are illustrated in Fig. 1. Two types of them are the model with a light scalar field: (I) the model with classical scale invariance (CSI), (II) the model without CSI. The last type of the model is (III) the model with the  $N$ -plet scalar field with TeV scale. These models can realize the EWSB via (I) radiative symmetry breaking, (II) Higgs mechanism and (III) EFT description of EWSB, respectively. For the simplicity of excluding the mixing terms, we assume  $Z_2$  symmetry in such a way that the new scalar field is  $Z_2$  odd while the others are  $Z_2$  even.

### A. The model with classical scale invariance

In the first type of the model, we impose CSI on the tree-level potential without any dimensional parameters, then the spontaneous EWSB is generated by radiative corrections [258] given later in (23). The Lagrangian of this model is

$$\mathcal{L} = \mathcal{L}_{\text{SM}} + |D_\mu \Phi_2|^2 - V_0(\Phi_1, \Phi_2), \quad (3)$$

where  $D_\mu = \partial_\mu - igT^a W_\mu^a - ig'Y_{\Phi_2} B_\mu/2$ ,  $g'$  and  $g$  are  $U(1)_Y$  and  $SU(2)_I$  gauge couplings, respectively, and  $T^a$  is the matrix for the generator of  $SU(2)_I$ . The tree-level potential  $V_0(\Phi_1, \Phi_2)$  is given by

$$V_0(\Phi_1, \Phi_2) = \lambda_1 |\Phi_1|^4 + \lambda_2 |\Phi_2|^4 + \lambda_{12} |\Phi_1|^2 |\Phi_2|^2. \quad (4)$$

If the isospin  $I_{\Phi_2}$  is  $1/2$ , then there are some mixing terms in the potential, such as  $|\Phi_1^\dagger \Phi_2|^2$ . For simplicity, we neglect such terms in the potential. According to Refs. [259, 260], there may be a flat direction in the tree-level potential to assure the valid perturbative analysis. If not, the large logarithmic term may show up in the one-loop correction via the renormalization scale, for example, this scale in the  $\phi^4$  theory is  $Q \sim 3\lambda v e^{16\pi^2}$  [258]. Therefore we assume a flat direction in the tree-level potential to avoid invalidating the perturbative analysis. The details of the effective potential will be discussed in Sec. III.

We mention here the constraints on this model. For simplicity, we assume that the additional scalar field  $\Phi_2$  does not couple to the SM fermions and does not have the vacuum-expectation-value (VEV). On the other hand, the isospin  $N$ -plet scalar field  $\Phi_2$  can interact with the SM gauge bosons. Then, the model is constrained by the perturbative unitarity bound. According to Ref. [261], the isospin should be less than  $7/2$ . We assume that the additional scalar field does not couple to the SM-like fermion in our strategy. Therefore, the typical collider constraints on our model is not much tight. For the neutral heavy Higgs, since it does not mix with the SM Higgs and does not couple to the SM fermions, the only experimental constraint comes from the vector boson scattering process, and thus it is very loose. For the charged Higgses, due to their degenerate masses to the neutral one, experimental constraints can be relaxed except for  $h\gamma\gamma$  measurement. The additional charged scalar fields contribute to the Higgs coupling  $h\gamma\gamma$  [262], which is given by  $1.05 \pm 0.09$  [263]. We may distinguish the models I and II by the results of measurements and observation of GW spectrum. In our work, we do not take into account the experimental constraints in the numerical analysis of the PT.

### B. The model without classical scale invariance

In the model without CSI, there are mass parameters in the tree-level potential. The tree-level potential in this model is given as

$$V_0(\Phi_1, \Phi_2) = -\mu_1^2 |\Phi_1|^2 - \mu_2^2 |\Phi_2|^2 + \lambda_{12} |\Phi_1|^2 |\Phi_2|^2 + \lambda_1 |\Phi_1|^4 + \lambda_2 |\Phi_2|^4, \quad (5)$$

where  $\mu_1^2 > 0$  and  $\lambda_1, \lambda_2 > 0$  for the stability of the tree-level potential. The effective potential of this model will be given later in (39).

Before discussing the effective potential with loop-

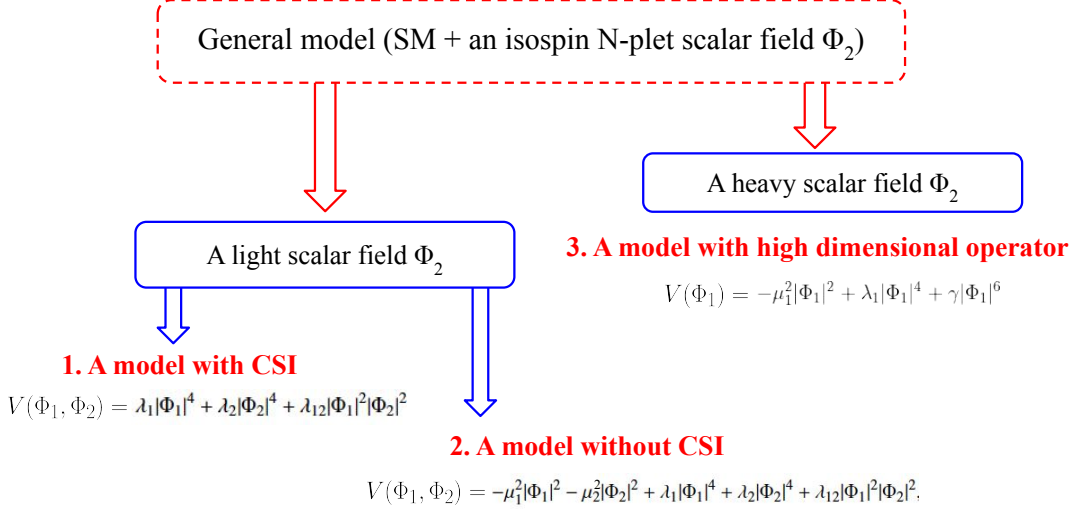


FIG. 1. Our effective model description for some BSM models with FOPTs from a general model with an additional scalar field, which is either light or heavy consisting of (I) the light scalar model with CSI, (II) the light scalar model without CSI, (III) the heavy scalar model with high dimensional operator.

corrections, we show the possible PT paths from the tree-level potential. At first, the extremal values in the potential are obtained by

$$\frac{\partial V_0(\langle \Phi_1 \rangle, \langle \Phi_2 \rangle)}{\partial \langle \Phi_1 \rangle} = \frac{\partial V_0(\langle \Phi_1 \rangle, \langle \Phi_2 \rangle)}{\partial \langle \Phi_2 \rangle} = 0, \quad (6)$$

which are solved by the following nine points in the field space as shown in Fig. 2,

$$\begin{aligned} (\langle \Phi_1 \rangle, \langle \Phi_2 \rangle) &= (0, 0), \quad \left(0, \pm \sqrt{\frac{\mu_2^2}{\lambda_2}}\right), \quad \left(\pm \sqrt{\frac{\mu_1^2}{\lambda_1}}, 0\right), \\ &\left(\pm \sqrt{2 \frac{\lambda_{12} \mu_2^2 - 2 \lambda_2 \mu_1^2}{\lambda_{12}^2 - 4 \lambda_1 \lambda_2}}, \pm \sqrt{2 \frac{\lambda_{12} \mu_2^2 - 2 \lambda_2 \mu_1^2}{\lambda_{12}^2 - 4 \lambda_1 \lambda_2}}\right), \\ &\left(\pm \sqrt{2 \frac{\lambda_{12} \mu_2^2 - 2 \lambda_2 \mu_1^2}{\lambda_{12}^2 - 4 \lambda_1 \lambda_2}}, \mp \sqrt{2 \frac{\lambda_{12} \mu_2^2 - 2 \lambda_2 \mu_1^2}{\lambda_{12}^2 - 4 \lambda_1 \lambda_2}}\right). \end{aligned} \quad (7)$$

The green point is the origin in the potential, the blue points are  $\langle \Phi_2 \rangle \neq 0$  at zero temperature and red and magenta points are along  $\langle \Phi_1 \rangle$  and  $\langle \Phi_2 \rangle$  axes, respectively. When the red or blue point is minimum, the scalar field  $\Phi_1$  can have a VEV. In this work, we especially focus on the one-step phase transition along  $\langle \Phi_1 \rangle$  axis, because this path is the same as the CSI case. To realize the phase transition, we assume that the red point is global minimum and the blue point is not minimum. We can assure such a situation by using the conditions for the determinants of the Hesse matrix and height of the potential. The determinants of the Hesse matrix at the red,

magenta and blue points are given by

$$\det[\mathcal{H}_{red}] = \mu_1^2 \left( \frac{\lambda_{12} \mu_1^2}{\lambda_1} - 2\mu_2^2 \right), \quad (8)$$

$$\det[\mathcal{H}_{mag}] = \mu_2^2 \left( \frac{\lambda_{12} \mu_2^2}{\lambda_2} - 2\mu_1^2 \right), \quad (9)$$

$$\det[\mathcal{H}_{blue}] = -4 \frac{(\lambda_{12} \mu_2^2 - 2\lambda_2 \mu_1^2)(\lambda_{12} \mu_1^2 - 2\lambda_1 \mu_2^2)}{\lambda_{12}^2 - 4\lambda_1 \lambda_2}. \quad (10)$$

Also, the height of the potential at these points are given by

$$V_0 \left( 0, \sqrt{\mu_2^2 / \lambda_2} \right) = -\mu_2^4 / 4\lambda_2, \quad (11)$$

$$V_0 \left( \sqrt{\mu_1^2 / \lambda_1}, 0 \right) = -\mu_1^4 / 4\lambda_1$$

$$\begin{aligned} V_0 \left( \sqrt{2 \frac{\lambda_{12} \mu_2^2 - 2 \lambda_2 \mu_1^2}{\lambda_{12}^2 - 4 \lambda_1 \lambda_2}}, \sqrt{2 \frac{\lambda_{12} \mu_2^2 - 2 \lambda_2 \mu_1^2}{\lambda_{12}^2 - 4 \lambda_1 \lambda_2}} \right) \\ = \frac{\lambda_1 \mu_2^4 + \lambda_2 \mu_1^4 - \lambda_{12} \mu_1^2 \mu_2^2}{\lambda_{12}^2 - 4 \lambda_1 \lambda_2}. \end{aligned} \quad (12)$$

The red point should be the lowest points among them. From that, we can obtain the following conditions

$$\frac{\lambda_{12} \mu_1^2}{\lambda_1} > 2\mu_2^2, \quad \frac{\lambda_{12} \mu_2^2}{\lambda_2} > 2\mu_1^2, \quad \mu_2^4 / \lambda_2 < \mu_1^4 / \lambda_1. \quad (13)$$

Since the potential with these conditions have two minima at magenta and red points, two-step phase transi-

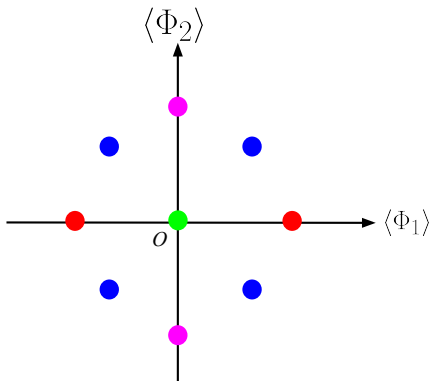


FIG. 2. The extreme values of the tree-level potential of the model without CSI given by Eq. (7). In our analysis, the red (magenta) points will be global (local) minimum points and the blue points are saddle points.

tion may be realized. In our numerical analysis, we distinguish the phase transition pattern and focus on the one-step phase transition to compare differences of the results between the models with and without CSI.

### C. The model with dimension-six operator from $\Phi_2$

In the last type of model,  $\Phi_2$  is assumed at the TeV scale and then we integrate out the additional scalar field. The tree-level potential in this model is given by

$$V_0(\Phi_1, \Phi_2) = -\mu_1^2 |\Phi_1|^2 - \mu_2^2 |\Phi_2|^2 + \lambda_1 |\Phi_1|^4 + \lambda_2 |\Phi_2|^4 + \lambda_{12} |\Phi_1|^2 |\Phi_2|^2, \quad (14)$$

where  $\mu_2$  is at TeV scale. Otherwise it is the same as the model without CSI. Then, we integrate out the heavy  $\Phi_2$  by loop-level matching [248, 264] in our analysis, and the effective Lagrangian for the SM-like Higgs boson  $h$  reads

$$\mathcal{L}_{\text{EFT}}^{(6)} \sim \frac{1}{2} |\partial_\mu h|^2 - \left( -\frac{1}{2} a_2 h^2 + \frac{1}{4} a_4 h^4 + \frac{1}{6} a_6 h^6 \right) \quad (15)$$

with

$$a_2 = \mu_1^2, \quad (16)$$

$$a_4 = \lambda_1 - (1 + 2I_{\Phi_2}) \frac{\lambda_{12}^2 \mu_1^2}{9(4\pi)^2 m_{\Phi_2}^2}, \quad (17)$$

$$a_6 = (1 + 2I_{\Phi_2}) \frac{1}{(4\pi)^2 m_{\Phi_2}^2} \left( \frac{\lambda_{12}^3}{8} + \frac{\lambda_{12}^2 \lambda_1}{6} \right), \quad (18)$$

where  $m_{\Phi_2}^2 = \mu_2^2 + \lambda_{12} v^2 / 2$  is the mass of the additional scalar field  $\Phi_2$ . The effective potential with radiative corrections of this model is given later in (51).

We note that Ref. [248] suggests FOPT may be difficult in the model with a loop-level matching. According to their work, the FOPT requires the balancing be-

tween the dimension-four and dimension-six terms via  $\frac{1}{4} \frac{U}{M^2} \frac{c_i \kappa^2}{16\pi^2} \sim \frac{m_h^2}{v^2} \sim 0.12$  with  $c_i = 1/2$  (1) for a real (complex) scalar, where  $U$  and  $M$  correspond to the Higgs boson coupling to the heavy field and the mass parameter of heavy field, respectively. On the other hand, the parameter region for a valid EFT expansion requires  $2c_{kin} v^2 < 1/2$  and  $|a_8| v^2 / a_6 < 1$ , where  $c_{kin}$ ,  $a_6$  and  $a_8$  are high dimensional operators for kinetic term, dimension 6 and 8 terms, respectively. Since the conditions also limit to  $U/M^2$  and  $c_i \kappa^2 / 16\pi^2$ . Therefore, they concluded that the FOPT cannot be generated in the model. At this time, we do not take into account other higher dimensional operators involving with the kinetic term.

### III. EFFECTIVE POTENTIALS

In this section, we discuss the forms of the effective potentials for our three effective model descriptions. To obtain the effective potential, we use the  $\overline{\text{MS}}$  scheme to absorb the divergence parts. Typically, the effective potential at one-loop level reads

$$V_{\text{eff}}(\langle\Phi_1\rangle, \langle\Phi_2\rangle, T) = V_0 + \sum_i \frac{n_i}{64\pi^2} M_i^4(\langle\Phi_1\rangle, \langle\Phi_2\rangle) \times \left( \ln \left( \frac{M_i^2(\langle\Phi_1\rangle, \langle\Phi_2\rangle)}{Q^2} \right) - c_i \right) + \Delta V_T, \quad (19)$$

where  $M_i^2(\langle\Phi_1\rangle, \langle\Phi_2\rangle)$  is the field-dependent mass,  $n_i$  is the number of the degree of freedom,  $Q$  is the renormalization scale and  $c_i$  is  $3/2$  ( $i = \text{boson, fermion}$ ) or  $5/6$  ( $i = \text{gauge boson}$ ). The one-loop thermal contribution to the potential [265] is

$$\Delta V_T = \frac{T^4}{2\pi^2} \left\{ \sum_{i=\text{bosons}} n_i \int_0^\infty dx x^2 \times \ln \left[ 1 - \exp \left( -\sqrt{x^2 + M_i^2(\langle\Phi_1\rangle, \langle\Phi_2\rangle, T)/T^2} \right) \right] + \sum_{i=\text{fermions}} n_i \int_0^\infty dx x^2 \times \ln \left[ 1 + \exp \left( -\sqrt{x^2 + M_i^2(\langle\Phi_1\rangle, \langle\Phi_2\rangle, T)/T^2} \right) \right] \right\}. \quad (20)$$

Here, we take into account the resummation effect  $V_T^{\text{ring}}$  obtained by [266]

$$V_T^{\text{ring}} = \frac{T}{12\pi} \sum_{i=\text{bosons}} n_i \left( (M_i^2(\langle\Phi_1\rangle, \langle\Phi_2\rangle, 0))^{3/2} - (M_i^2(\langle\Phi_1\rangle, \langle\Phi_2\rangle, T))^{3/2} \right), \quad (21)$$

where the thermal mass  $M_i^2(\langle\Phi_1\rangle, \langle\Phi_2\rangle, T) = M_i^2(\langle\Phi_1\rangle, \langle\Phi_2\rangle) + \Pi_i$  receives the thermal correction from the thermal self-energy  $\Pi_i$ . Finally, the

effective potential with finite temperature effects is obtained by

$$V_{\text{eff}}(\langle\Phi_1\rangle, \langle\Phi_2\rangle, T) = V_0 + V_{1\text{-loop}} + \Delta V_T + V_T^{\text{ring}}. \quad (22)$$

The field-dependent masses in the effective potential of Eq. (19) and thermal correction  $\Pi_i$  in Eq. (22) depend on the details of model. Therefore we will discuss the form of effective potential in each type of the model in the following.

### A. The model with classical scale invariance

For the model (4) with CSI, the spontaneous EWSB occurs on the flat direction, which is assumed along  $\langle\Phi_1\rangle$ . Then, the effective potential is simply

$$V_{\text{eff}}(\varphi, T=0) = A\varphi^4 + B\varphi^4 \ln \frac{\varphi^2}{Q^2}, \quad (23)$$

with  $A$  and  $B$  terms given by

$$A = \sum_i \frac{n_i}{64\pi^2 v^4} m_i^4 \left( \ln \frac{m_i^2}{v^2} - c_i \right), \quad B = \sum_i \frac{n_i}{64\pi^2 v^4} m_i^4, \quad (24)$$

where  $m_i$  is the mass of the field species  $i$  excluding the Higgs boson since this effect is at one-loop level in this model case.  $n_i$  and  $c_i$  in the potential are given by  $(n_W, n_Z, n_t, n_{\Phi_2}) = (6, 3, -12, 2(2I_{\Phi_2} + 1))$  and  $(c_W, c_Z, c_t) = (5/6, 5/6, 3/2, 3/2)$ , respectively. Using the stationary condition, we have

$$\left. \frac{\partial V_{\text{eff}}(\varphi, T=0)}{\partial \varphi} \right|_{\varphi=v} = \ln \frac{v^2}{Q^2} + \frac{1}{2} + \frac{A}{B} = 0, \quad (25)$$

where the renormalization scale  $Q$  is fixed. Because  $A$  and  $B$  are the loop effects,  $v$  can be large in contrast to the case of  $\phi^4$  theory. Also, the Higgs boson mass is obtained as

$$m_h^2 = \left. \frac{\partial^2 V_{\text{eff}}(\varphi, T=0)}{\partial \varphi^2} \right|_{\varphi=v} = 8Bv^2, \quad (26)$$

from which we can obtain the additional scalar boson mass  $m_{\Phi_2}$  as

$$m_{\Phi_2} = \frac{C}{(2(2I_{\Phi_2} + 1))^{1/4}}, \quad (27)$$

$$C^4 \equiv 8\pi^2 v^2 m_h^2 - 3m_Z^4 - 6m_W^4 + 12m_t^4 \quad (28)$$

with  $C = 543 \text{ GeV}$  determined by Eq.(10) of Ref. [267], and  $\lambda_{12}$  coupling is obtained via  $m_{\Phi_2}^2 = \lambda_{12}v^2/2$  as

$$\lambda_{12} = \frac{\sqrt{2}C^2}{v^2 \sqrt{2I_{\Phi_2} + 1}}. \quad (29)$$

With the help of Eqs. (25) and (26), the one-loop effective potential at zero temperature could be obtained in terms of the renormalized mass of the Higgs boson as

$$V_{\text{eff}}(\varphi, T=0) = \frac{m_h^2}{8v^2} \varphi^4 \left( \ln \frac{\varphi^2}{v^2} - \frac{1}{2} \right). \quad (30)$$

Since the loop effects are renormalized into the Higgs boson mass, the value of  $hhh$  coupling with one-loop effects does not depend on the model extension [267]. The field-dependent masses and resummation effects in the effective potential with finite temperature effects are

$$M_{\Phi_2}^2(\varphi, T) = \frac{m_{\Phi_2}^2}{v^2} \varphi^2 + T^2 \left( (I_{\Phi_2} + 1) \frac{\lambda_2}{6} + \frac{m_{\Phi_2}^2}{3v^2} + I_{\Phi_2}(I_{\Phi_2} + 1) \frac{g^2}{4} + Y_{\Phi_2}^2 \frac{g'^2}{16} \right). \quad (31)$$

Similarly, the thermally corrected field-dependent masses of gauge bosons in the  $(W^1, W^2, W^3, B)$  basis are

$$M_g^{2(L,T)}(\varphi, T) = \frac{\varphi^2}{4} \begin{pmatrix} g^2 & & & \\ & g^2 & & \\ & & g^2 & gg' \\ & & gg' & g'^2 \end{pmatrix} + a_g^{(L,T)} T^2 \begin{pmatrix} \pi_W & & & \\ & \pi_W & & \\ & & \pi_W & \\ & & & \pi_B \end{pmatrix}, \quad (32)$$

where

$$M_W^2 = \frac{g^2}{4} \varphi^2, \quad M_{WB}^2 = \frac{gg'}{4} \varphi^2, \quad M_B^2 = \frac{g'^2}{4} \varphi^2, \quad (33)$$

$$\pi_W = \frac{g^2}{9} I_{\Phi_2} (1 + I_{\Phi_2}) (1 + 2I_{\Phi_2}) + \frac{11}{6} g^2, \quad (34)$$

$$\pi_B = \frac{g'^2 T^2}{12} (1 + I_{\Phi_2}) Y_{\Phi_2}^2 + \frac{11}{6} g'^2, \quad a_g^L = 1, \quad a_g^T = 0. \quad (35)$$

The field-dependent mass of fermion does not receive thermal correction in  $T^2$  so that

$$M_t^2 = \frac{m_t^2}{v^2} \varphi^2. \quad (36)$$

In this model, there are three parameters in the tree-level potential,

$$\lambda_1, \lambda_2, \lambda_{12}, \quad (37)$$

where  $\lambda_1$  is zero in order to assume a flat direction along  $\langle\Phi_1\rangle$  axis. According to Eq. (26), the isospin number  $I_{\Phi_2}$  is related to the mass  $m_{\Phi_2}$ . Therefore, the free parameters in the effective potential with finite temperature

effects are in fact

$$I_{\Phi_2}, Y_{\Phi_2}, \lambda_2. \quad (38)$$

### B. The model without classical scale invariance

For the model (5) without CSI, the effective potential is given by

$$V_{\text{eff}}(\varphi_1, \varphi_2, T) = V_0 + \sum_i \frac{n_i}{64\pi^2} M_i^4 \left( \ln \frac{M_i^2}{Q^2} - c_i \right) + \Delta V_T, \quad (39)$$

where  $\langle \Phi_1 \rangle = \varphi_1/\sqrt{2}$ ,  $\langle \Phi_2 \rangle = \varphi_2/\sqrt{2}$  and

$$V_0 = -\frac{\mu_1^2}{2}\varphi_1^2 - \frac{\mu_2^2}{2}\varphi_2^2 + \frac{\lambda_1}{4}\varphi_1^4 + \frac{\lambda_2}{4}\varphi_2^4 + \frac{\lambda_{12}}{4}\varphi_1^2\varphi_2^2. \quad (40)$$

There are the five model parameters in the tree-level potential and these parameters can be fixed in terms of following parameters,

$$v, m_h, m_{\Phi_2}, \lambda_{12}, \lambda_2, \quad (41)$$

by the stationary conditions and the second derivatives of the effective potential. The details of them are given in Appendix A.

The field-dependent masses with resummation corrections from the finite temperature effects of the effective potential are

$$M_{h,\Phi_2}^2(\varphi_1, \varphi_2, T) = \frac{1}{2} (M_{11}^2 + M_{22}^2 \mp \sqrt{(M_{11}^2 - M_{22}^2)^2 + 4M_{12}^2 M_{21}^2}), \quad (42)$$

$$M_{N_1}^2(\varphi_1, \varphi_2, T) = -\mu_1^2 + \lambda_1\varphi_1^2 + \frac{\lambda_{12}}{2}\varphi_2^2 + T^2 \left( (2I_{\Phi_2} + 1) \frac{\lambda_{12}}{12} + \frac{\lambda_h}{4} + \frac{3g^2}{16} + \frac{g'^2}{16} + \frac{y_t^2}{4} \right), \quad (43)$$

$$M_{N_2}^2(\varphi_1, \varphi_2, T) = -\mu_2^2 + \lambda_2\varphi_2^2 + \frac{\lambda_{12}}{2}\varphi_1^2 + T^2 \left( \frac{(I_{\Phi_2} + 1)\lambda_2}{6} + \frac{\lambda_{12}}{6} + \frac{g^2}{4} (I_{\Phi_2}^2 + I_{\Phi_2}) + \frac{g'^2 Y_{\Phi_2}^2}{16} \right), \quad (44)$$

where

$$\begin{pmatrix} M_{11}^2 & M_{12}^2 \\ M_{21}^2 & M_{22}^2 \end{pmatrix} = \begin{pmatrix} -\mu_1^2 + 3\lambda_1\varphi_1^2 + \frac{\lambda_{12}}{2}\varphi_2^2 & \lambda_{12}\varphi_1\varphi_2 \\ \lambda_{12}\varphi_1\varphi_2 & -\mu_2^2 + 3\lambda_2\varphi_2^2 + \frac{\lambda_{12}}{2}\varphi_1^2 \end{pmatrix} + T^2 \begin{pmatrix} (2I_{\Phi_2} + 1) \frac{\lambda_{12}}{12} + \frac{\lambda_1}{4} + \frac{3g^2}{16} + \frac{g'^2}{16} + \frac{y_t^2}{4} & 0 \\ 0 & \frac{(I_{\Phi_2} + 1)\lambda_2}{6} + \frac{\lambda_{12}}{6} + \frac{g^2}{4} (I_{\Phi_2}^2 + I_{\Phi_2}) + \frac{g'^2 Y_{\Phi_2}^2}{16} \end{pmatrix}. \quad (45)$$

Also the thermally corrected field-dependent masses of gauge bosons in the  $(W^1, W^2, W^3, B)$  basis are

$$M_g^{2(L,T)} = \begin{pmatrix} M_W^2 & & & \\ & M_W^2 & & \\ & & M_W^2 & M_{WB}^2 \\ & & M_{WB}^2 & M_B^2 \end{pmatrix} + a_g^{(L,T)} T^2 \begin{pmatrix} \pi_W & & & \\ & \pi_W & & \\ & & \pi_W & \\ & & & \pi_B \end{pmatrix}, \quad (46)$$

where

$$M_W^2 = \frac{g^2}{4} (\varphi_1^2 + I_W^2 \varphi_2^2), \quad M_{WB}^2 = \frac{gg'}{4} (\varphi_1^2 + Y_{\Phi_2}^2 \varphi_2^2), \quad (47)$$

$$M_B^2 = \frac{g'^2}{4} (\varphi_1^2 + Y_{\Phi_2}^2 \varphi_2^2), \quad a_g^L = 1, \quad a_g^T = 0, \quad (48)$$

$$\pi_W = \frac{g^2}{9} I_{\Phi_2} (1 + I_{\Phi_2}) (1 + 2I_{\Phi_2}) + \frac{11}{6} g^2, \quad (49)$$

$$\pi_B = \frac{g'^2 T^2}{12} (1 + I_{\Phi_2}) Y_{\Phi_2}^2 + \frac{11}{6} g'^2. \quad (50)$$

In this model, the EWPT can be generated in multi-field space  $(\varphi_1, \varphi_2)$ . We will focus on the path of the phase transition along  $\varphi_1$  axis. Therefore, we will discuss the possibility of one-step and two-step PTs, and will especially focus on the path of the phase transition along  $\varphi_1$  axis to discuss the distinction among the three types of models with one-step PT.

### C. The model with dimension-six operator from $\Phi_2$

For the effective model (15) after integrating out the heavy scalar sector from (14), the effective potential is

$$V_{\text{eff}}(\varphi_1, T) = -\frac{1}{2}a_2\varphi_1^2 + \frac{1}{4}a_4\varphi_1^4 + \frac{1}{6}a_6\varphi_1^6 + \sum_i \frac{n_i}{64\pi^2} M_i^4 \left( \ln \left( \frac{M_i^2}{Q^2} \right) - c_i \right) + \Delta V_T, \quad (51)$$

where  $a_2$ ,  $a_4$  and  $a_6$  are given in Eq. (16), and the field-dependent mass of Higgs boson along with its thermal correction are

$$M_h^2(\varphi_1) = -a_2 + 3a_4\varphi_1^2 + 5a_6\varphi_1^4, \quad (52)$$

$$\Pi_h = T^2 \left( \frac{a_4}{4} + \frac{3g^2}{16} + \frac{g'^2}{16} + \frac{y_t^2}{4} \right). \quad (53)$$

The thermally corrected field-dependent masses of gauge bosons in the  $(W^1, W^2, W^3, B)$  basis are

$$M_g^{2(L,T)}(\varphi, T) = \frac{\varphi^2}{4} \begin{pmatrix} g^2 & & & \\ & g^2 & & \\ & & g^2 & gg' \\ & & gg' & g'^2 \end{pmatrix} + a_g^{(L,T)} T^2 \begin{pmatrix} \pi_W & & & \\ & \pi_W & & \\ & & \pi_W & \\ & & & \pi_B \end{pmatrix}, \quad (54)$$

where

$$M_W^2 = \frac{g^2}{4}\varphi_1^2, \quad M_{WB}^2 = \frac{gg'}{4}\varphi_1^2, \quad M_B^2 = \frac{g'^2}{4}\varphi_1^2, \quad (55)$$

$$\pi_W = \frac{11}{6}g^2, \quad \pi_B = \frac{11}{6}g'^2, \quad a_g^L = 1, \quad a_T = 0 \quad (56)$$

and the field-dependent mass of top quark is

$$M_t^2 = \frac{m_t^2}{v^2}\varphi_1^2. \quad (57)$$

There are three new parameters in this potential, namely,

$$m_{\Phi_2}^2, \lambda_{12}, I_{\Phi_2}. \quad (58)$$

## IV. GRAVITATIONAL WAVES

The GWs from the FOPTs serve as the promising probe for the new physics of BSM, including our EFT models of EWSB. In this section, we briefly outline the computation procedures to carry out our model constraints.

### A. Phase-transition parameters

For an effective potential  $V_{\text{eff}}$  exhibiting a false vacuum  $\phi_+$  and a true vacuum  $\phi_-$  separated by a potential barrier, a cosmological FOPT proceeds via stochastic nucleations of true vacuum bubbles followed by a rapid expansion until a successful percolation to fully complete the phase transition process. In this section, we describe the phase transition dynamics consisting of the bubble nucleation and bubble percolation, which could be determined by the thermodynamics of effective potential alone without reference to the microscopic physics that leads to the macroscopic hydrodynamics of bubble expansion.

#### Bounce action

The bubble nucleations of true vacuum bubbles at finite temperature admit stochastic emergences of the field configuration  $\phi(r)$  connecting a true vacuum region  $\phi(r=0) \equiv \phi_0 \lesssim \phi_-$  (assuming  $\phi_+ < \phi_-$ ) to the asymptotic false vacuum region  $\phi(r \rightarrow \infty) \equiv \phi_+$  in an  $O(4)$ -symmetric manner  $ds^2 = dr^2 + r^2 d\Omega_3^2$  or an  $O(3)$ -symmetric manner  $ds^2 = d\tau^2 + dr^2 + r^2 d\Omega_2^2$  depending on their maximum value of the nucleation rates [268–271]

$$\Gamma(T) = \max \left[ T^4 \left( \frac{S_3}{2\pi T} \right)^{\frac{3}{2}} e^{-\frac{S_3}{T}}, \frac{1}{R_0^4} \left( \frac{S_4}{2\pi} \right) e^{-S_4} \right], \quad (59)$$

where the  $O(4)$  bounce action

$$S_4 = 2\pi^2 \int_0^\infty dr r^3 \left[ \frac{1}{2} \left( \frac{d\phi_B}{dr} \right)^2 + V_{\text{eff}}(\phi_B, T) - V_{\text{eff}}(\phi_+, T) \right] \quad (60)$$

is evaluated at the solution  $\phi_B$  of the equation-of-motion

$$\frac{d^2\phi}{dr^2} + \frac{3}{r} \frac{d\phi}{dr} = \frac{\partial V_{\text{eff}}}{\partial \phi}, \quad \phi'(0) = 0, \quad \phi(\infty) = \phi_+, \quad (61)$$

while the  $O(3)$  bounce action

$$\frac{S_3}{T} = \frac{4\pi}{T} \int_0^\infty dr r^2 \left[ \frac{1}{2} \left( \frac{d\phi_B}{dr} \right)^2 + V_{\text{eff}}(\phi_B, T) - V_{\text{eff}}(\phi_+, T) \right] \quad (62)$$

is evaluated at the solution  $\phi_B$  of the equation-of-motion

$$\frac{d^2\phi}{dr^2} + \frac{2}{r} \frac{d\phi}{dr} = \frac{\partial V_{\text{eff}}}{\partial \phi}, \quad \phi'(0) = 0, \quad \phi(\infty) = \phi_+. \quad (63)$$

In the realistic estimations, the vacuum decay rate from  $S_4$  usually dominates over the thermal decay rate from  $S_3/T$  at extremely low temperature when the potential barrier does not vanish even at  $T=0$ .  $R_0$  is the bubble radius defined by  $\phi_B(r=R_0) = (\phi_0 - \phi_+)/2$ .

### Nucleation temperature

During the whole process of bubble nucleation, the false vacuum becomes unstable once the temperature drops below the critical temperature defined by

$$V_{\text{eff}}(\phi_+, T_c) = V_{\text{eff}}(\phi_-(T_c), T_c). \quad (64)$$

However, the bubble nucleation is only possible when the temperature further drops down to  $T = T_i < T_c$  defined

$$\phi_B(r = 0, T_i) = \phi_-(T_i) \quad (65)$$

due to the presence of the Hubble friction term in the bounce equation. Since then, one can count the number of nucleated bubbles in one Hubble volume during a given time elapse by

$$N(T(t)) = \int_{t_i}^t dt \frac{\Gamma(t)}{H^3} = \int_T^{T_i} \frac{dT}{T} \frac{\Gamma(T)}{H(T)^4}, \quad (66)$$

until the nucleation temperature  $T_n < T_i$  defined by the moment when there is exactly one bubble nucleated in one Hubble volume,

$$N(T_n) = 1. \quad (67)$$

### Percolation temperature

The progress of the phase transition could be described by the the expected volume fraction of the true-vacuum regions at time  $t$  [272–274],

$$I(t) = \frac{4\pi}{3} \int_{t_i}^t dt' \Gamma(t') a(t')^3 r(t, t')^3, \quad (68)$$

where  $r(t, t')$  is the comoving radius of a bubble at  $t$  nucleated at an earlier time  $t'$ ,

$$r(t, t') \equiv \frac{R_0}{a(t')} + \int_{t'}^t \frac{v_w(\tilde{t}) d\tilde{t}}{a(\tilde{t})} \approx v_w \int_{t'}^t \frac{d\tilde{t}}{a(\tilde{t})}. \quad (69)$$

Here we omit the initial bubble radius  $R_0$  and fix the time-dependent bubble wall velocity  $v_w(t)$  at its terminal  $v_w$ . When the effects for the overlapping of true-vacuum bubbles and “virtual bubbles” nucleated in the true-vacuum regions are taken into account, the fraction of regions that are still sitting at the false vacuum at time  $t$  could be approximated by the exponentiation of  $I(t)$ ,

$$P(t) = e^{-I(t)}. \quad (70)$$

A percolation temperature  $T_p < T_n$  is therefore defined by a conventional estimation [24, 122, 274–276]

$$P(T_p) = 1/e. \quad (71)$$

In what follows, the strength factor and characteristic length scale for determining the peak amplitude and frequency in the GW spectrum will be evaluated at the percolation temperature.

### Strength factor

To characterize the total released latent heat into the plasma, a parameter  $\alpha$  is defined by [274]

$$\alpha(T) = \frac{\Delta\rho_{\text{vac}}(T)}{\rho_{\text{rad}}(T)}, \quad (72)$$

with the total released vacuum energy defined by

$$\begin{aligned} \Delta\rho_{\text{vac}}(T) &= \rho(\phi_+, T) - \rho(\phi_-(T), T) \\ &= \Delta V_{\text{eff}}(T) - T \frac{\partial \Delta V_{\text{eff}}(T)}{\partial T} \end{aligned} \quad (73)$$

due to  $\rho = \mathcal{F} + Ts = -p + T \frac{\partial p}{\partial T} = V_{\text{eff}} - T \frac{\partial V_{\text{eff}}}{\partial T}$  similar to the usual definition of latent heat  $L(T_c) = \rho(\phi_+, T_c) - \rho(\phi_-(T_c), T_c)$  at critical temperature. Here  $\Delta V_{\text{eff}}(T) \equiv V_{\text{eff}}(\phi_+(T), T) - V_{\text{eff}}(\phi_-(T), T)$  for short.

### Characteristic length scale

The characteristic length scale  $R_*$  for the peak position of the GW spectrum is estimated from the inverse duration  $\beta$  of the phase transition via the average number density of bubbles as

$$R_* = n_B^{-1/3} = (8\pi)^{1/3} v_w \beta^{-1}, \quad (74)$$

where the inverse duration  $\beta$  of the phase transition is computed by expanding the nucleation rate around the percolation time,

$$\Gamma = e^{\beta(t-t_p)+\dots}, \quad P(t_p) = 1/e, \quad (75)$$

$$\beta = - \left. \frac{d}{dt} \frac{S_3(t)}{T(t)} \right|_{t=t_p} = H(T) T \left. \frac{d}{dT} \frac{S_3(T)}{T} \right|_{T=T_p}. \quad (76)$$

## B. Gravitational wave spectrum

The GW spectrum from a FOPT consists of three contributions: the bubble wall collisions, the sound waves, and the MHD turbulences. The contribution from the MHD turbulences is usually sub-dominated and hence omitted in the current study. The contribution from the bubble wall collisions [277–281] only dominates the total GW spectrum when the bubble walls collide with each other while they are still rapidly accelerating. In most of the cases, the runaway wall expansion is highly unlikely, and they usually collide with each other long after having approached to the terminal velocity. Therefore, we only

consider the contribution from the sound waves, which is well fitted numerically by [282–285][274, 286]

$$h^2\Omega_{\text{sw}} = 8.5 \times 10^{-6} \left(\frac{100}{g_{\text{dof}}}\right)^{\frac{1}{3}} \left(\frac{\kappa_v \alpha}{1 + \alpha}\right)^2 \left(\frac{H_*}{\beta}\right) v_w \frac{7^{\frac{7}{2}} (f/f_{\text{sw}})^3}{\left(4 + 3 (f/f_{\text{sw}})^2\right)^{\frac{7}{2}}} \Upsilon(\tau_{\text{sw}}), \quad (77)$$

with the peak frequency

$$f_{\text{sw}} = 1.9 \times 10^{-5} \text{ Hz} \left(\frac{g_{\text{dof}}}{100}\right)^{\frac{1}{6}} \frac{T_*}{100 \text{ GeV}} \frac{1}{v_w} \frac{\beta}{H_*}. \quad (78)$$

Here the suppression factor  $\Upsilon$  is only important for sufficiently long duration comparable to or even slightly larger than the Hubble time scale, which is also neglected in our current study. Furthermore, both the wall velocity  $v_w$  and efficiency factor of bulk fluid motions  $\kappa_v$  are also set to be unity for simplicity.

To quickly locate the parameter space with a promising detectability of the GW signals, we will first use the ratio  $\phi_C/T_C$  at the critical temperature as a roughly estimation for the size of the strength factor [4, 287],

$$\alpha \sim \alpha_\infty \simeq 4.9 \times 10^{-3} \left(\frac{\phi_*}{T_*}\right)^2, \quad (79)$$

which is a typically reliable estimation for most of the non-supercooling electroweak PTs since there are no new relativistic degrees of freedom or new particles with couplings to the Higgs comparable to those of the  $SU(2)_L$  gauge bosons or top quark. To qualify the model detectability, the GWs signals  $h^2\Omega_{\text{GW}}(f)$  are compared to the sensitivity curves of some GW detectors  $h^2\Omega_{\text{sen}}(f)$  during the mission year  $\mathcal{T}$  by the signal-to-noise ratio (SNR),

$$\text{SNR} = \sqrt{\mathcal{T} \int_{f_{\text{min}}}^{f_{\text{max}}} df \left[ \frac{h^2\Omega_{\text{GW}}(f)}{h^2\Omega_{\text{sen}}(f)} \right]^2}. \quad (80)$$

## V. SUMMARY OF RESULTS

In this section, we show the results for the effective model descriptions with three types of the EWSB: (I) the light scalar model with CSI, (II) the light scalar model without CSI, and (III) the heavy scalar model with a higher dimensional operator after integrating out the additional heavy scalar. Besides the common SM parameters ( $v, m_h, m_W, m_Z, m_t, g, g', \alpha_s, y_t$ ), the new parameters in these three models are summarized below:

- For model I, there are five parameters ( $I_{\Phi_2}, Y_{\Phi_2}, \lambda_1, \lambda_2, \lambda_{12}$ ) from the effective potential (23). By using the stationary condition, we can introduce the massive parameter EW vacuum by the dimensional transmutation [258]. From

the second derivative of the potential, the  $\lambda_{12}$  is related to the SM effects, like Eq. (29).  $\lambda_1$  is assumed to be zero for a flat direction along  $\langle \Phi_1 \rangle$  axis. Eventually, there are three free dimensionless parameters: ( $I_{\Phi_2}, Y_{\Phi_2}, \lambda_2$ ).

- For model II, there are seven parameters ( $I_{\Phi_2}, Y_{\Phi_2}, \mu_1, \mu_2, \lambda_1, \lambda_2, \lambda_{12}$ ) in the effective potential. With the stationary condition, the massive parameter  $\mu_1$  can be replaced by the EW VEV  $v$ . From the second derivatives of the potential,  $\lambda_1$  and  $\mu_2$  parameters are given by the Higgs boson mass  $m_h$  and the additional scalar boson mass  $m_{\Phi_2}$ . Eventually, there are five free parameters: ( $I_{\Phi_2}, Y_{\Phi_2}, \lambda_2, m_{\Phi_2}, \lambda_{12}$ ).
- For model III, there are five parameters ( $I_{\Phi_2}, \mu_1, m_{\Phi_2}, \lambda_1, \lambda_{12}$ ) from the tree-level potential (15), two of which, for example,  $\mu_1$  and  $\lambda_1$ , could be fixed by the EW vacuum normalization conditions in terms of the EW VEV  $v$  and the Higgs mass  $m_h$ , leaving behind three free parameters ( $I_{\Phi_2}, m_{\Phi_2}, \lambda_{12}$ ).

Note that in the models I and II, although the hypercharge  $Y_{\Phi_2}$  is a free parameter, it does not significantly change the PT results since its effect is proportional to  $(m_W - m_Z)$  via Daisy diagram contributions. Thus, we take  $Y_{\Phi_2} = 1$  as an illustrative example in the following PT analysis. For consistent comparison, we consider the models with common values for the shared free parameters. For example, the model I and model II can be compared in the parameter space of  $I_{\Phi_2}$  and  $\lambda_2$  for given choices of  $m_{\Phi_2}$  and  $\lambda_{12}$  as illustrated in Fig. 3. The black plane in Fig. 3 corresponds to the parameter region for model I. The  $m_{\Phi_2}$  is proportional to the  $\lambda_{12}$  in this model. Such a relation is given by a line in the plane of  $(m_{\Phi_2}, \lambda_{12})$ . Since the  $\lambda_2$ , which corresponds to the  $z$  axis in this figure, is independent free parameter, the black plane in Fig. 3 corresponds to the parameter region for model I. The green lines are the  $I_{\Phi_2}$  in the model I. Since the model II has five free parameters, the all free parameters in this model cannot be determined, even if the parameters have the same values as the CSI model. Such parameter regions corresponds to the red and blue planes.

### A. The model with classical scale invariance

In this section, we first show the value of  $\phi_C/T_C$  for the model I in the first panel of Fig. 4 to see which part of parameter space could produce detectable GWs. The horizontal axis is the quartic coupling  $\lambda_2$  and the vertical axis is the isospin  $I_{\Phi_2}$  of the additional scalar boson fields. It is easy to see that the value of  $\phi_C/T_C$  is large for either small isospin  $I_{\Phi_2}$  or small  $\lambda_2$  coupling. This result of  $\phi_C/T_C$  is different from our intuition since the strongly FOPT can be typically realized by adding a large number

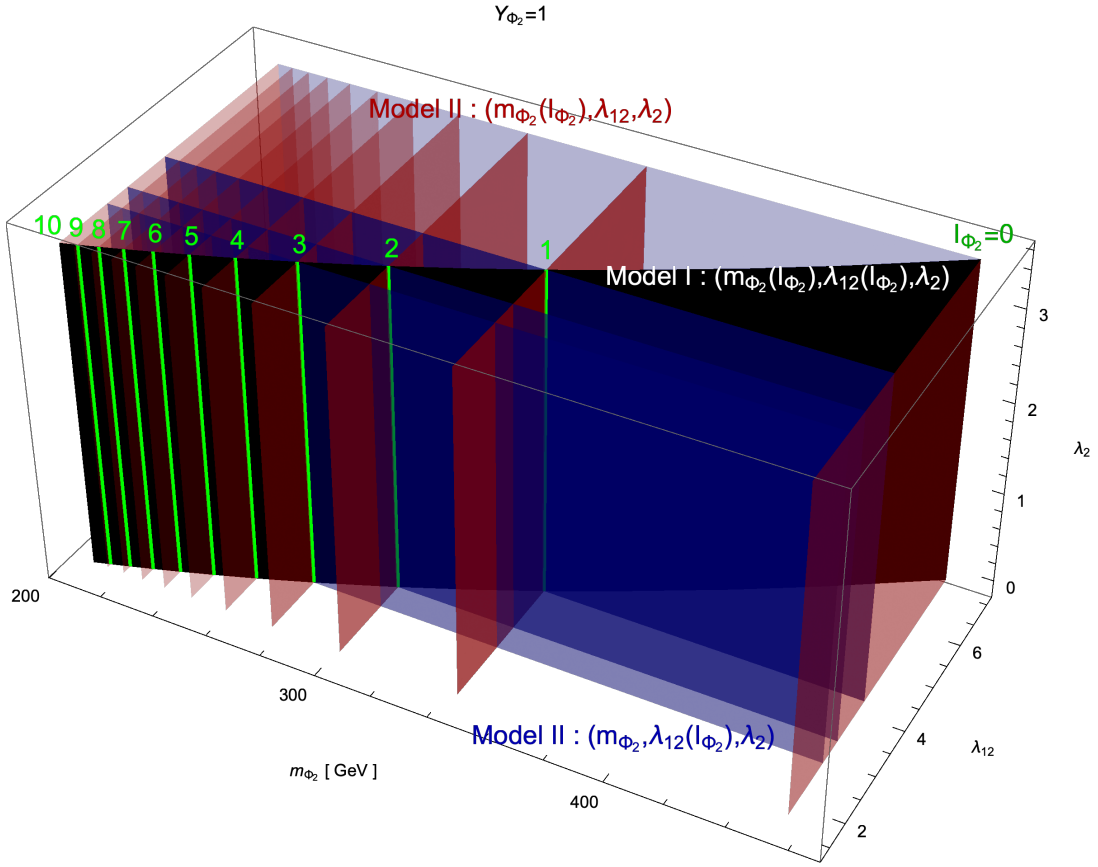


FIG. 3. The presentation for a part of the effective models of interest in the parameter space supported by  $(m_{\Phi_2}, \lambda_{12}, \lambda_2)$  with a fixed  $Y_{\Phi_2} = 1$ . The black strip is the model I with both  $m_{\Phi_2}$  and  $\lambda_{12}$  determined by  $I_{\Phi_2}$  labeled in green. For model II, we take two illustrative examples with (1) the same  $m_{\Phi_2}$  as the model I but a free  $\lambda_{12}$  detached from  $I_{\Phi_2}$  presented as red slices, and (2) the same  $\lambda_{12}$  as the model I but a free  $m_{\Phi_2}$  detached from  $I_{\Phi_2}$  presented as blue slices.

of additional scalar boson fields into the model, which corresponds to a large isospin  $I_{\Phi_2}$ . In the model with CSI, the number of additional scalar boson fields is related to the Higgs boson mass via Eq. (26). Then, the  $\phi_C/T_C$  without ring diagram contribution is roughly estimated by

$$\frac{\phi_C}{T_C} = \frac{E}{\lambda_2} \propto I_{\Phi_2}^{1/4}. \quad (81)$$

On the other hand, the ring diagram contribution has  $I_{\Phi_2}^2$ -dependence in Eq. (45), therefore,  $\phi_C/T_C$  becomes small through large ring diagram contributions from large  $I_{\Phi_2}^2$  value.

The PT parameters  $T_n$ ,  $\alpha$  and  $\beta/H$  are shown in the last three panels of Fig. 4, respectively. From these parameters, we can describe the GW spectrum from the FOPT. The SNR for the testability of this model with CSI is shown in Fig. 5 with respect to the future spaceborne GW detectors LISA, DECIGO, and BBO. When evaluating the SNR, we simply take the mission duration to be one year and the bubble wall velocity to be one. The red dashed curves in the panels of DECIGO and BBO represent SNR=10. In the parameter regions to

the left of the red dashed curves, the SNR is larger than 10, therefore, these parameter regions could be tested at future GW detectors DECIGO and BBO. From these figures, most of parameter regions for the model with CSI could be tested by the DECIGO and BBO missions.

## B. The model without classical scale invariance

In this section, we show the results for the model II, which admits two more free parameters than the model I, namely,  $m_{\Phi_2}$  and  $\lambda_{12}$ . To compare with model I/III with only one-step PT (the additional VEV does not appear in the potential at zero temperature), we will focus on the parameter regions where the same one-step PT for model II as model I/III (green  $\rightarrow$  red in Fig. 2) can be realized. We also neglect the parameter regions with other paths of PT, for example, two-step PT (namely the path along green  $\rightarrow$  magenta  $\rightarrow$  red, where the red is a global minimum). We numerically examine the parameter regions where one-step EWPT can be generated by using following four parameter regions: (i) the same  $m_{\Phi_2}$  and  $\lambda_{12}$  as the model I, (ii) the same  $m_{\Phi_2}$  as model I,

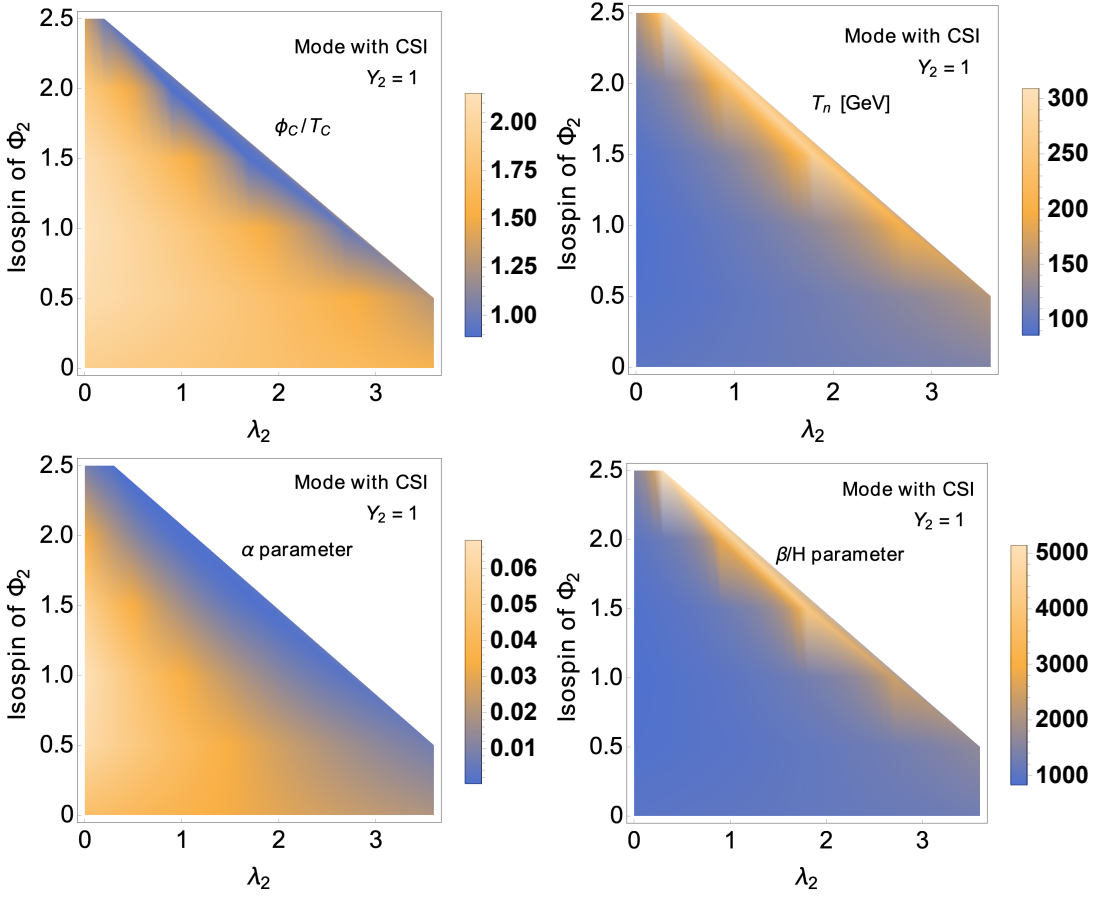


FIG. 4. The values of  $\phi_c/T_c$ ,  $T_n$ ,  $\alpha$  and  $\beta/H$  for the model I with respect to  $\lambda_2$  coupling and isospin  $I_{\Phi_2}$  of the additional scalar boson fields.

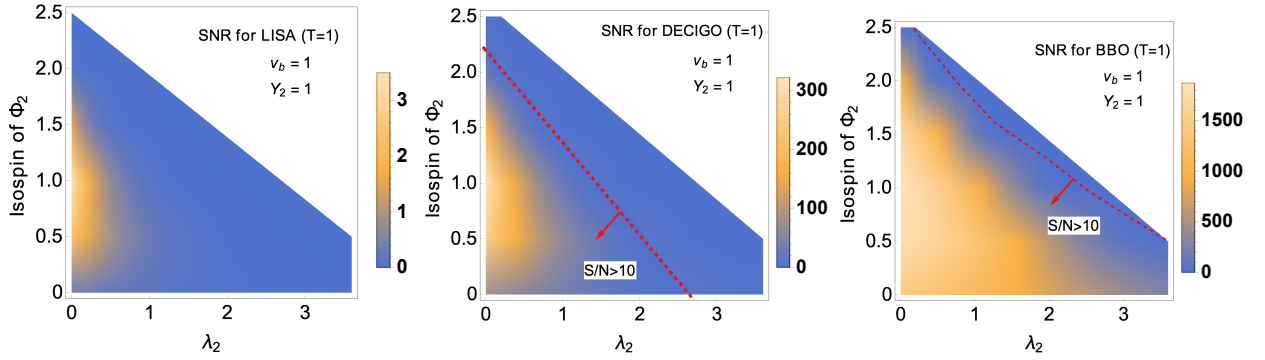


FIG. 5. The values of SNR for the model with CSI at LISA, DECIGO and BBO. The experimental period is one year and bubble wall velocity is 1. The red dashed line represents  $\text{SNR}=10$ .

(iii) the same  $m_{\Phi_2}$  as model III, and (iv) different  $m_{\Phi_2}$  and  $\lambda_{12}$  from other models.

In the parameter region (i), there are the minimum points along  $\varphi_1$  and  $\varphi_2$  axes at the black-point region in Fig. 6, but the minimum points along  $\varphi_1$  and  $\varphi_2$  axes are local and global minima, respectively. According our numerical results, the two-step PT (green  $\rightarrow$  red  $\rightarrow$  ma-

genta) is generated at the black-point region, and the magenta point becomes the true vacuum. In such a case, we cannot explain the fermion mass since the additional scalar field  $\Phi_2$  does not couple to the fermion fields anymore. Therefore, in the parameter (i) for the model II, we cannot realize a proper PT which can make up the current universe. Although the model I can generate the

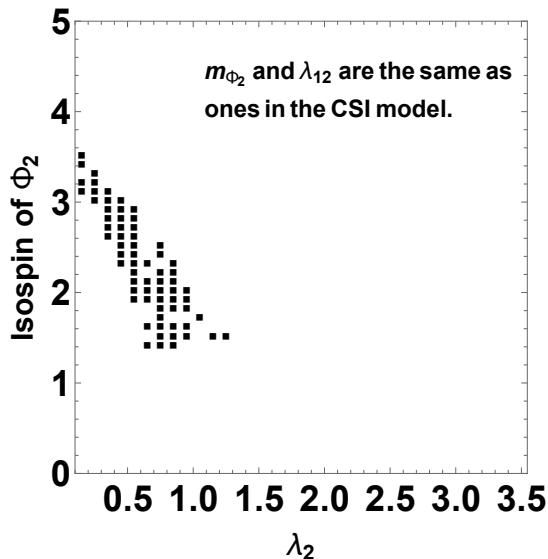


FIG. 6. The parameter region can have a stable minimum point along  $\varphi_1$  and  $\varphi_2$  axes. At these black points, there is global minimum along  $\varphi_2$  axis.

detectable GW from the one-step EWPT in Fig. 5, the model II cannot realize the correct PT between green and red points in the parameter region (i), which shares the same parameter values as the model I. Therefore, we can distinguish the models with and without CSI by the GW detection.

In the parameter case (ii), model II admits the same  $m_{\Phi_2}$  given by Eq. (27) as the model I but with  $\lambda_{12} = 1.5, 2.0, 2.5, 3.0$  decoupled from  $I_{\Phi_2}$  by Eq. (29) as shown in Fig. 7, respectively. Note that in the case of model I,  $m_{\Phi_2}$  and  $\lambda_{12}$  are related by  $m_{\Phi_2}^2 = \lambda_{12}v^2/2$ , and thus we can get almost the same results for a similar case with the same  $\lambda_{12}$  as model I by Eq. (29) but decoupled  $m_{\Phi_2}$  from  $I_{\Phi_2}$  by Eq. (27). All colored points in Fig. 7 admit their global minimum along  $\varphi_1$  (namely the red point in Fig. 2). To show the parameter region where one-step PT along  $\varphi_1$  axis can be generated, we compare the critical temperatures for the PT along  $\varphi_1$  and  $\varphi_2$  axes. From the numerical results, the blue points in Fig. 7 have higher critical temperature for the PTs along  $\varphi_2$  than the PT for  $\varphi_1$ . On the other hand, the green and red points in Fig. 7 can realize the one-step PT (green  $\rightarrow$  red in Fig. 2), especially, the red points can realize the strong FOPT along  $\varphi_1$  axis where the detectable GWs may be generated. At these red points in the model with  $\lambda_{12} = 2$  and  $2.5$ , the SNR for BBO with mission time  $\mathcal{T}=1$  yr and  $v_b = 1$  is larger than 10. Furthermore, the SNR for DECIGO with mission time  $\mathcal{T}=1$  yr and  $v_b = 1$  at  $(\lambda_2, I_{\Phi_2})=(0.25, 0.5)$  is about 10.87, while other red points have their SNR no more than 10 for DECIGO. In short summary, a small  $\lambda_2$  is necessary for detectable GWs in the model II, which is not necessary for the model I as shown in Fig. 5.

To compare the results between the model II and the model III, we show the results in the parameter region (iii) with heavy  $m_{\Phi_2}$  as model III. For example, the results for heavy  $m_{\Phi_2} = 650$  GeV with some  $\lambda_2$  values in the model II are shown in Fig. 8, however, the effects from the additional heavy scalar field decouple. From the additional scalar mass  $M_{\Phi_2}(\varphi)^2 \sim -\mu_2^2 + \lambda_{12}\varphi^2$  with large  $\mu_2^2$  value, the cubic term of field-dependent mass in the effective potential can be expanded like  $(M_{\Phi_2}^2)^{3/2} \sim |\mu_2^3| + \lambda_{12}\mu_2\varphi^2 + \lambda_{12}^2\varphi^4/\mu_2$ , but the cubic  $\varphi^3$  term does not appear in the potential. On the other hand, the  $M_{\Phi_2}(\varphi)^{3/2}$  with small  $\mu_2^2$  value can have  $\lambda_{12}^{3/2}\varphi^3$  as the source of a barrier. Therefore, it is difficult to generate a sizable barrier to realize first-order EWPT in the model II with much heavy additional scalar field. For the large negative  $\mu_2^2$  term, the one-step PT occurs between green and red points in Fig. 2. In this case,  $\lambda_2$ , which is the coefficient of  $\Phi_2^4$ , does not much affect the EWPT, and the results are not very different between two figures of Fig. 8.

The first two panels in Fig. 9 represent the results in the model with  $\lambda_{12}=3$  and  $m_{\Phi_2} = 650$  and  $425$  GeV, which correspond to the parameter regions (iii) and (iv), respectively. With these parameters, the mass parameter  $\mu_2$  becomes small (non-decoupling) and the detectable GW spectrum can be generated. Especially, in the model with  $m_{\Phi_2} = 425$  GeV, the red (magenta) marks can be described in the upper right figure, and the SNR for DECIGO (BBO) is larger than 10. The last panel in Fig. 9 represents the results with respect to  $I_{\Phi_2}$  and  $m_{\Phi_2}$ , which are related to parameter region (iv) in the model with benchmark parameters  $\lambda_2 = 0.5$  and  $\lambda_{12} = 2.5$ . The blue marks in this model can realize two-step PT. In short summary, the detectable GWs, which are represented by red and magenta marks, can be produced in the massive model with small isospin of  $\Phi_2$  and small  $\lambda_2$  value. However, for the model II, such parameter regions with detectable GWs are not the same as those in model I and model III. Therefore we may distinguish the three types of models by the GW observations.

### C. The model with dimension-six operator from $\Phi_2$

In this section, we discuss the testability for the model III. At first, the parameter region of  $a_6$  is shown in Fig. 10 for detectable GWs at DECIGO and BBO with mission duration  $\mathcal{T} = 1$  yr and  $v_b = 1$ . In the dark regions, the SNR is smaller than 10, hence we require for a large  $a_6$  value. Recall that with Eq. (16),  $a_6 = (1 + 2I_{\Phi_2}) \frac{1}{(4\pi)^2 m_{\Phi_2}^2} \left( \frac{\lambda_{12}^3}{8} + \frac{\lambda_{12}^2 \lambda_1}{6} \right)$ , a large  $a_6$  value generally prefers a large isospin  $I_{\Phi_2}$ , namely a large number of the additional scalar boson fields. We should further check the conditions for a valid EFT expansion  $|a_8|v^2/a_6 < 1$  and  $2c_{kin}v^2 < 1/2$ , which was discussed in

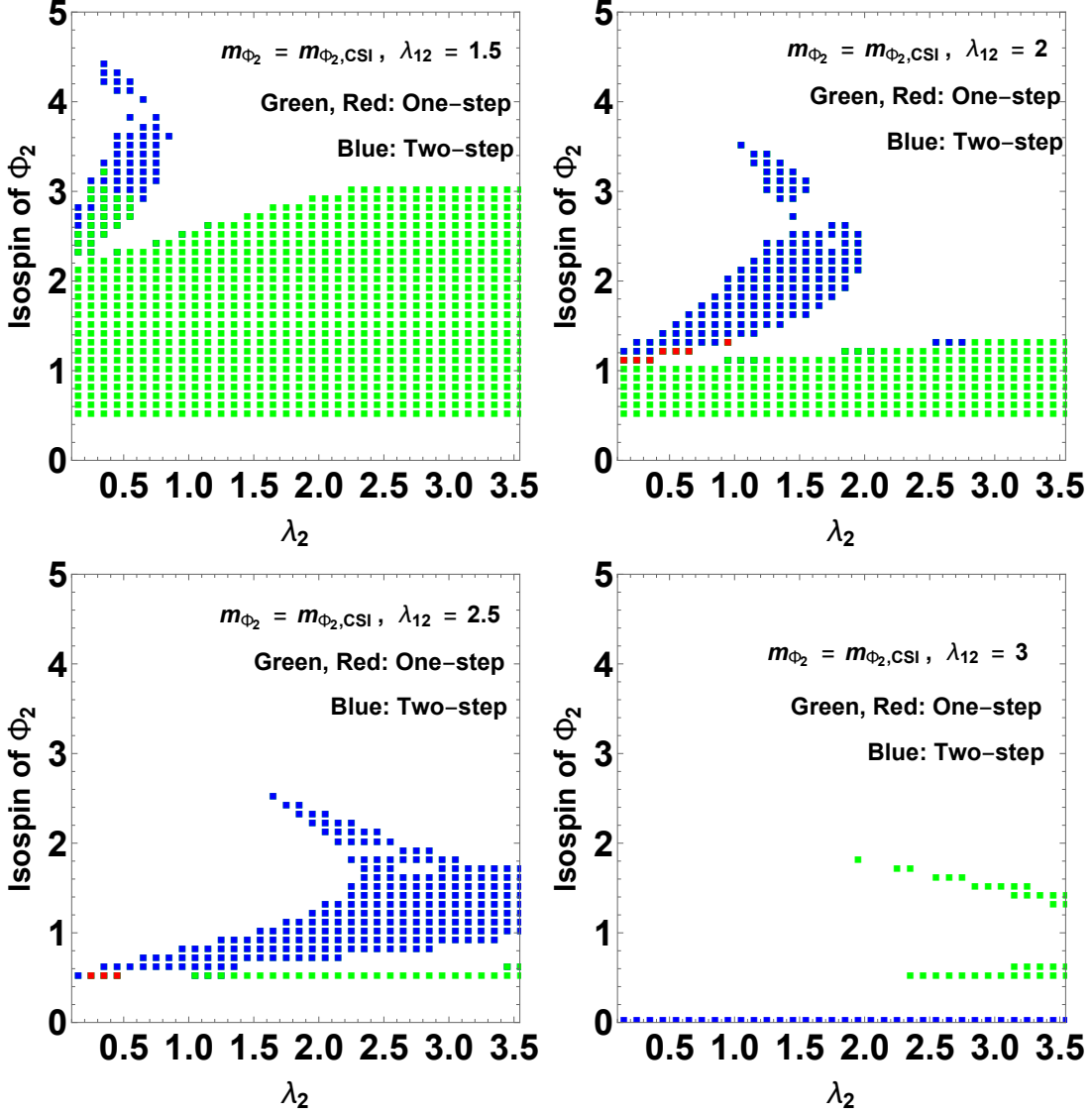


FIG. 7. Different PT regions in the parameter space supported by  $\lambda_2$  and  $\Phi_2$  for the model II with the same  $m_{\Phi_2}$  as the model I but allowing for different  $\lambda_{12} = 1.5, 2.0, 2.5, 3.0$ . The blue points represent the two-step PT. The red and green points represent the one-step PT. The detectable GWs at the BBO detection can be generated for the red points. For the rest of regions in this figure, the global minimum point does not appear along  $\varphi_1$  axis otherwise the potential is unstable.

Ref. [248]. In this model III, these conditions are

$$\frac{\lambda_{12}v^2}{2m_{\Phi_2}^2} < 1, \quad (1 + 2I_{\Phi_2}) \frac{\lambda_{12}^2v^2}{12(4\pi)^2m_{\Phi_2}^2} < 1. \quad (82)$$

The left and right panels of Fig. 11 represents the values of the light hand side of these conditions. The left panel is the comparison between dimension 6 and 8 operators. Since the operators has one-loop level effects, the isospin  $I_{\Phi_2}$  cancel in this relation. On the other hand, the right panel is the comparison between tree-level and one-loop level, therefore the value of this relation depends on the isospin  $I_{\Phi_2}$ . For the presented parameter space, the conditions for a valid EFT expansion can be satisfied.

The values of  $\phi_C/T_C$ ,  $T_n$ ,  $\alpha$  and  $\beta/H$  are then shown in Fig. 12 and the corresponding SNR at DECIGO and BBO are shown in Fig. 13, where the parameter regions to the right of red dashed lines have their SNR larger than 10. However, SNR is less than  $10^{-5}$  for LISA, hence LISA may be difficult to test the parameter region of the model III. For detectable GWs from the model III, we require a large number of additional scalar fields (namely a large isospin  $I_{\Phi_2}$ ) and large coupling  $\lambda_{12}$ , which can be distinguished from models I and II by detectable GWs in the parameter regions of small isospin  $I_{\Phi_2}$ . In particular, the model I cannot take the heavy scalar field with  $m_{\Phi_2} = 650$  GeV since the additional scalar mass should be less than 543 GeV from Eq. (27) [267]. Therefore, we may

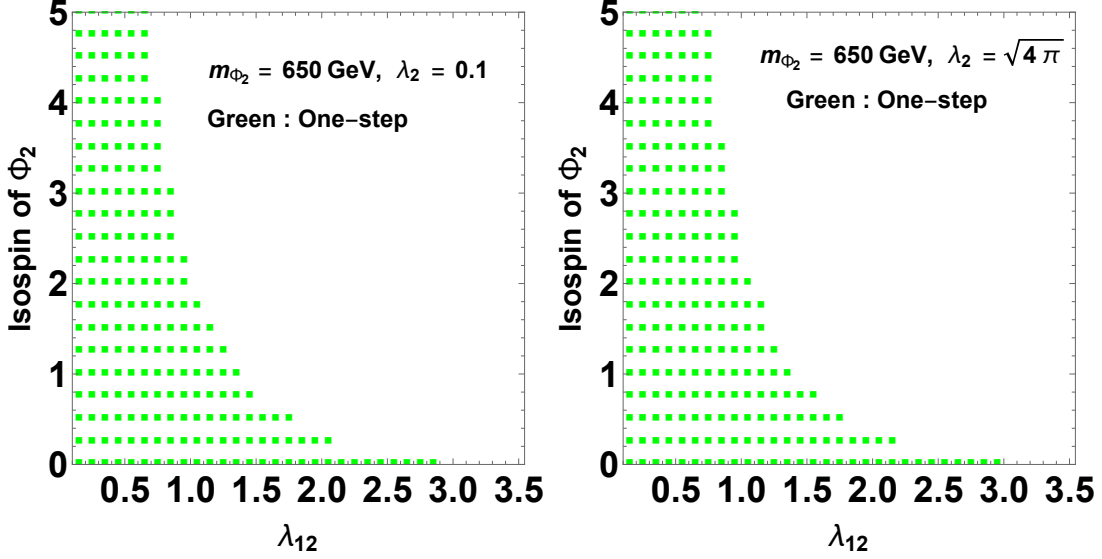


FIG. 8. The model parameters for the model II with  $\lambda_2 = 0.1, \sqrt{4\pi}$  and  $m_{\Phi_2} = 650$  GeV. The horizontal axis in left and right figures is  $\lambda_{12}$ . Otherwise, the same as Fig. 7.

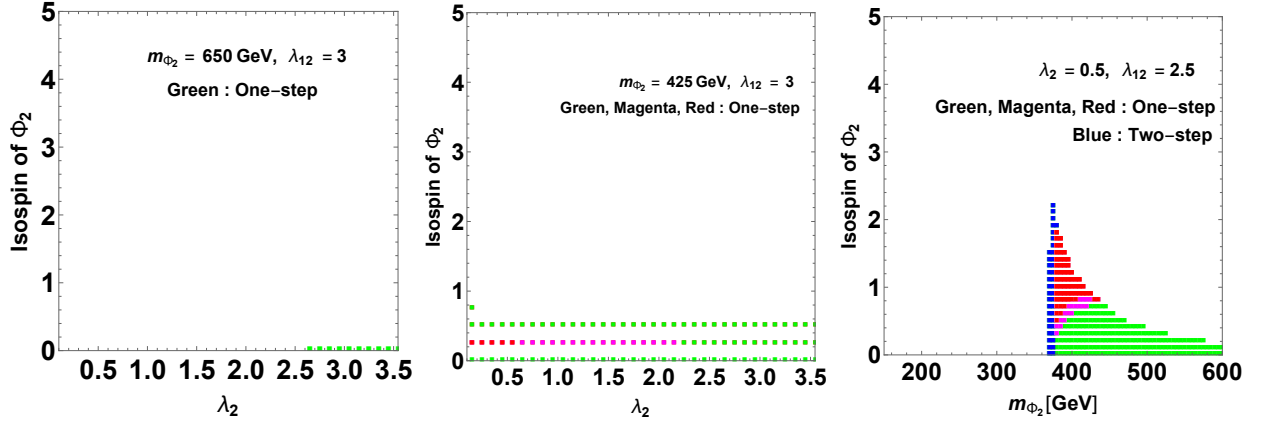


FIG. 9. (First two panels) The model parameters for the model II with  $\lambda_{12} = 3$  and  $m_{\Phi_2} = 650, 425$  GeV in the upper left and upper right panels, respectively. At the red (magenta) marks, the detectable GWs at DECIGO (BBO) can be generated. Otherwise, the same as Fig. 7. (Last panel) The results in the model with  $\lambda_2 = 0.5$  and  $\lambda_{12} = 2.5$ . Horizontal axis is the additional scalar boson mass. The two-step PT occurs at blue marks.

distinguish the model III from model I and model II by constraining the isospin of additional scalar fields with the GWs background observed at future GW detectors.

## VI. CONCLUSIONS AND DISCUSSIONS

The predictions for the GW background vary sensitively among different concrete models but also share a large degeneracy in the model buildings. From that, in this time, we take into account an EFT treatment for three BSM models based on different patterns of the EWSB: (I) classical scale invariance, (II) generic scalar

extension, and (III) higher dimensional operators. In these EFTs, the EWSB can be realized by (I) radiative symmetry breaking, (II) Higgs mechanism, and (III) EFT description of EWSB, respectively.

These three models can realize the strongly first-order EWPT and can produce the detectable GW spectrum by the effects summarized in Tab. II. Here,  $C_n$  are the effective couplings of the order parameter operators  $\phi^n$  in the effective potential. The dominant contributions of  $\lambda_2$  and  $I_{\Phi_2}$  in models (I) and (II) show up through the ring diagram effects as shown in Eqs (31), (34), (45) and (47). Thus, a small  $\lambda_2$  and a small  $I_{\Phi_2}$  are required to produce the detectable GW spectrum. The differences

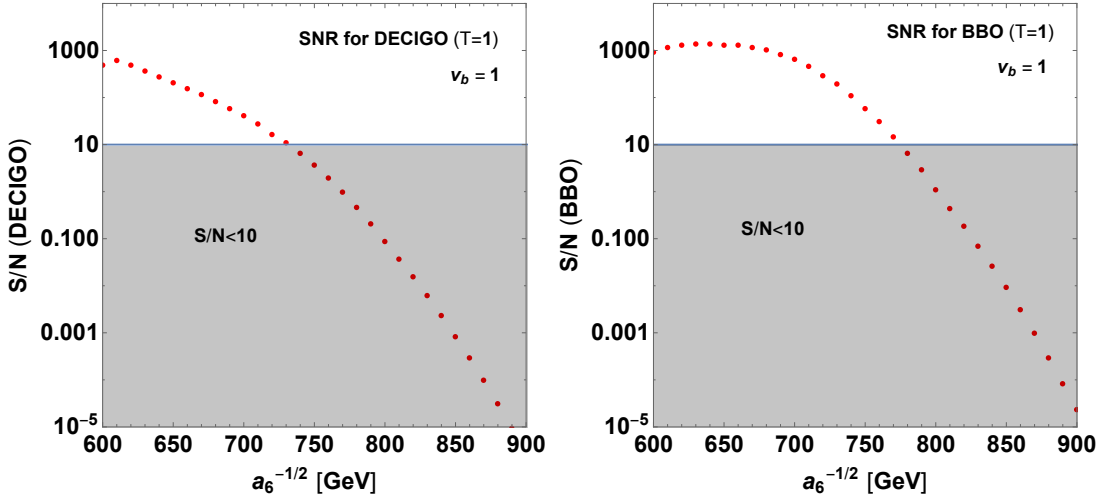


FIG. 10. The SNR value from the model with a higher dimensional operator for DECIGO and BBO with mission year  $\mathcal{T} = 1$  yr and  $v_b = 1$ .

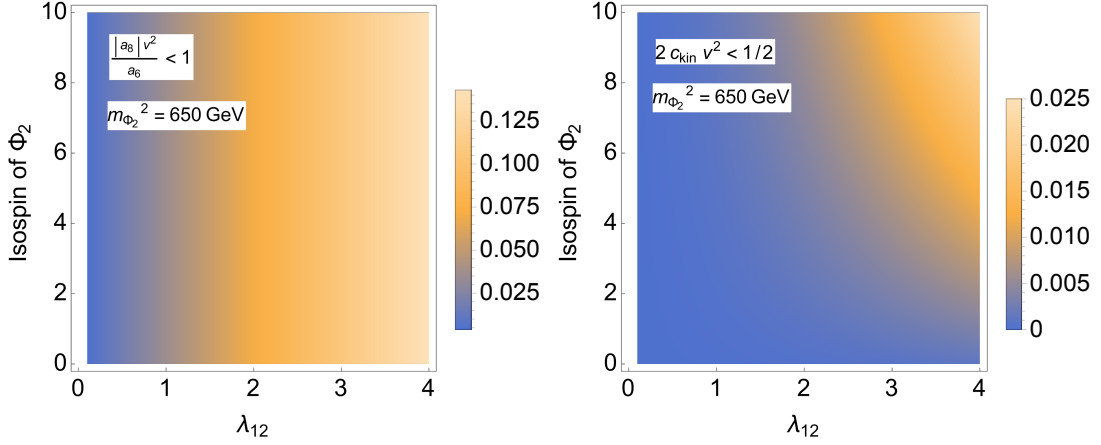


FIG. 11. The valid EFT expansion  $2c_{kin}v^2 < 1/2$  and  $|a_8|v^2/a_6 < 1$  in the model with a higher dimensional operator with respect to  $I_{\Phi_2}$  and  $\lambda_{12}$  and fixed  $m_{\Phi_2} = 650$  GeV. Since the first condition comes from the comparison between one-loop dimension 6 and 8 operators, the values do not depend on the isospin  $I_{\Phi_2}$ . For the presented parameter regions, the conditions for a valid EFT expansion can be satisfied.

between models (I) and (II) are the  $C_2$  and  $C_4$  terms and the number of free parameters in the model. In the model (II), these terms have the tree-level contribution, and thus we need to tune model parameters to have a sizable  $C_3$  comparable with these  $C_2$  and  $C_4$  terms. Unlike the model (I), we can use the  $\lambda_{12}$  parameter to realize such a situation and could generate the first-order EWPT as shown in Fig. 7. On the other hand, the  $\lambda_2$  in model (III) does not contribute to the effective potential after integrating out the  $\Phi_2$  scalar field, and the high dimensional operator  $a_6^{-1/2}$  in Fig. 10 is inversely proportional to  $\lambda_{12}$  and  $I_{\Phi_2}$  as shown in Eq. (16). Therefore, a small  $a_6^{-1/2}$  can be realized by a large  $\lambda_{12}$  and a large  $I_{\Phi_2}$ .

These three types of models might be distinguished by investigating the detectable GWs in the parameter

Model	$C_2\phi^2$	$C_3\phi^3$	$C_4\phi^4$	$C_6\phi^6$	GW features
I	Loop	Loop	Loop	None	Small $\lambda_2$ and small $I_{\Phi_2}$
II	Tree	Loop	Tree	None	Small $\lambda_2$ and small $I_{\Phi_2}$
III	Tree	Loop	Tree	Tree	Large $\lambda_{12}$ and large $I_{\Phi_2}$

TABLE II. The potential forms in the three types of the models where the EWSB can be realized by (I) radiative symmetry breaking, (II) Higgs mechanism and (III) EFT description of EWSB, respectively. The last column shows the source of detectable GW spectrum in these models. Otherwise, the same as Tab. I.

regions with overlapping parameters: (1) Model I and model II might be distinguished by the detection of GWs

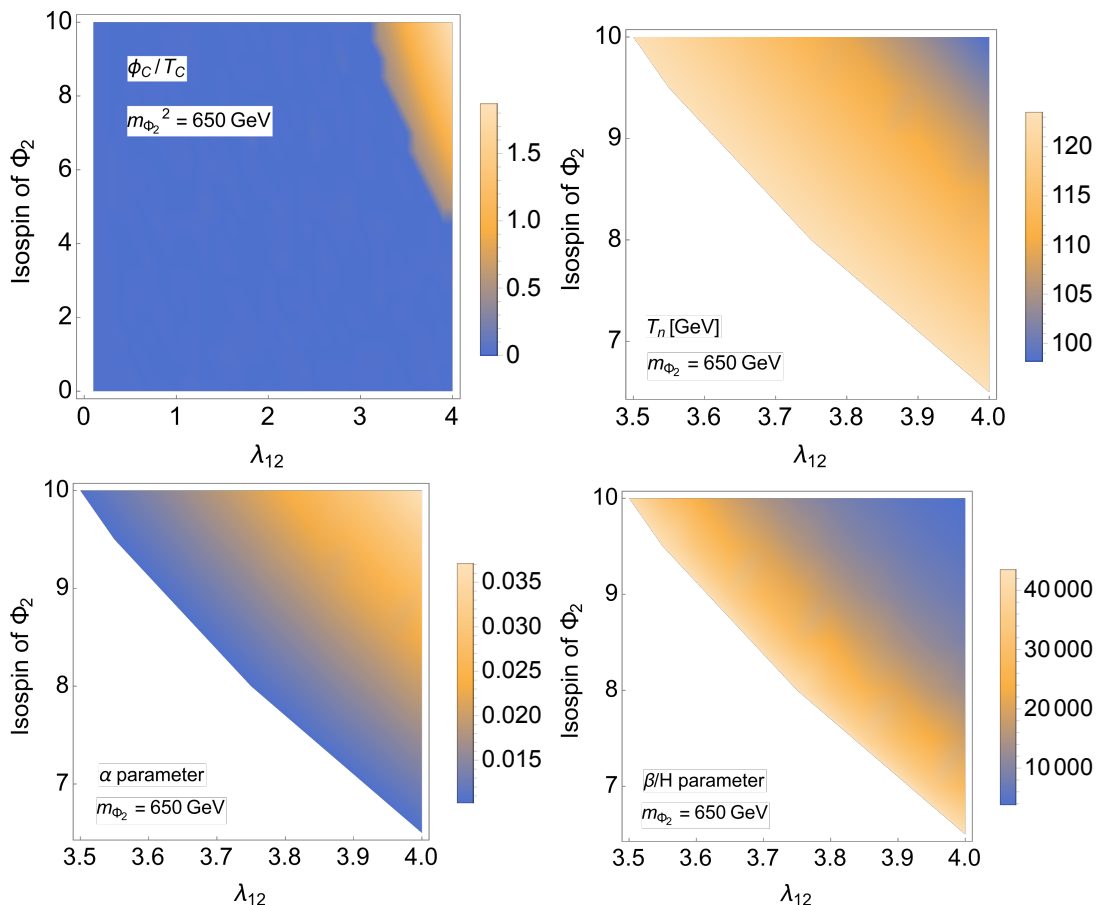


FIG. 12. The value of  $\phi_C/T_C$ ,  $T_n$ ,  $\alpha$  and  $\beta/H$  in the EFT model with  $m_{\Phi_2} = 650$  GeV. Otherwise, the same as Fig. 11.

in the parameter regions as shown in Figs. 5 and 6. When taking the same  $m_{\Phi_2}$  and  $\lambda_{12}$  as model I by Eqs. (27) and (29), model II cannot generate the correct one-step PT where the red point in Fig. 2 is the local minimum. However, when just taking the same  $m_{\Phi_2}$  as model I by Eq. (27) but decoupling  $\lambda_{12}$  from  $I_{\Phi_2}$  by Eq. (29), model II could produce detectable GWs in the parameter regions of small  $\lambda_2$  and small  $I_{\Phi_2}$ , which is partially overlapping with model I with detectable GWs. In this case, although we cannot fully distinguish models I and II by the GW detections alone, we may use other observations, such as  $hhh$  coupling [172] and  $h\gamma\gamma$  coupling [262, 267], to do that. (2) Model II and model III can be distinguished by the detection of GWs in the parameter regions as shown in Figs. 8 and 13 since detectable GWs are produced for model II in the parameter regions of small  $\lambda_2$  and small  $I_{\Phi_2}$ , while model III favors a large  $I_{\Phi_2}$  to generate detectable GWs. (3) Similarly, model I could also be distinguished from model III by detectable GWs in the parameter regions of small  $I_{\Phi_2}$  (model I) and large  $I_{\Phi_2}$  (model III). Furthermore, the additional scalar mass should be less than 543 GeV in the model I, different from the case of model III with a heavy scalar field.

Therefore, we may distinguish these three effective model descriptions of EWPT by future GW detections in space. Nevertheless, our PT analysis for the effective model descriptions is preliminary in surveying part of the parameter space, and it only depicts those scalar extensions (with  $Z_2$  symmetry) of fundamental Higgs models [288–290] and Coleman-Weinberg Higgs models [267, 291, 292], but by no means covers all the effective models of EWPT. We will investigate the PT dynamics in a more general classifications of EWSB [293] in the ever-enlarging parameter space in future works.

## ACKNOWLEDGMENTS

This work is mainly supported by the National Key Research and Development Program of China Grant No. 2021YFC2203004, No. 2021YFA0718304, and No. 2020YFC2201501, R. G. C. is supported by the National Natural Science Foundation of China Grants No. 11947302, No. 11991052, No. 11690022, No. 11821505 and No. 11851302, the Strategic Priority Research Program of the Chinese Academy of Sciences (CAS) Grant No. XDB23030100, No. XDA15020701, the Key Research

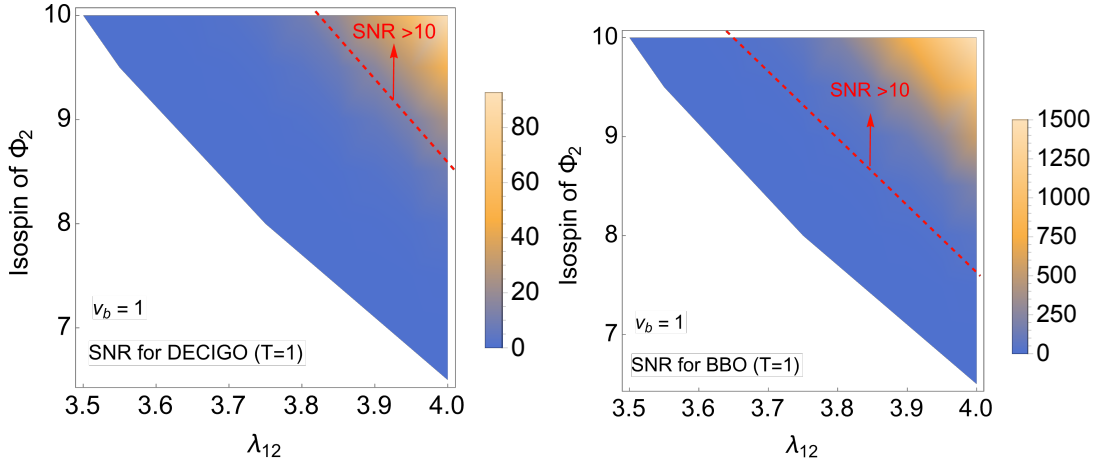


FIG. 13. The values of SNR in the EFT model with  $m_{\Phi_2} = 650$  GeV at DECIGO and BBO. The ratio of SNR is larger than 10 in the parameter region to right of the red dashed lines.

Program of the CAS Grant No. XDPB15, the Key Research Program of Frontier Sciences of CAS. S. J. W. is supported by the National Key Research and Development Program of China Grant No. 2021YFC2203004, No. 2021YFA0718304, the National Natural Science Foundation of China Grant No. 12422502, No. 12105344, the China Manned Space Project with NO.CMS-CSST-2021-B01. J. H. Y. is supported by the National Science Foundation of China under Grants No. 12022514, No. 11875003 and No. 12047503, and National Key Research and Development Program of China Grant No. 2020YFC2201501, No. 2021YFA0718304, and CAS Project for Young Scientists in Basic Research YSBR-006, the Key Research Program of the CAS Grant No.

XDPB15.

#### Appendix A: Stationary condition and CP-even boson masses in the model without CSI

We use the stationary condition at  $(\varphi_1, \varphi_2) = (v, 0)$  and the second derivatives of the potential with one-loop effects,

$$\left. \frac{\partial V_{eff}}{\partial \langle \Phi_1 \rangle} \right|_{\langle \Phi_1 \rangle=v, \langle \Phi_2 \rangle=0} = 0, \quad \left. \frac{\partial^2 V_{eff}}{\partial \langle \Phi_1 \rangle^2} \right|_{\langle \Phi_1 \rangle=v, \langle \Phi_2 \rangle=0} = m_h^2, \quad (\text{A1})$$

where we take  $Q = v = 246$  GeV. With tadpole condition  $\mathcal{M}_{\Phi_2\Phi_2}^2 > \mathcal{M}_{\Phi_1\Phi_1}^2$ , one arrives at

$$\begin{aligned} \left. \frac{\partial V_{eff}}{\partial \langle \Phi_1 \rangle} \right|_{\langle \Phi_1 \rangle=v, \langle \Phi_2 \rangle=0} &= -\mu_1^2 + \lambda_1 v^2 + \frac{1}{16\pi^2} \left[ \frac{6\lambda_1 + \lambda_{12}}{4} f_+(m_{\Phi_{1,r}}^2, m_{\Phi_{2,r}}^2) + \frac{1}{4} (6\lambda_1 - \lambda_{12}) f_-(m_{\Phi_{1,r}}^2, m_{\Phi_{2,r}}^2) \right. \\ &\quad + (2(2I_{\Phi_2} - 1) - 1) \frac{\lambda_{12} m_{N_{2,r}}^2}{2} \left( \ln \frac{m_{N_{2,r}}^2}{Q^2} - 1 \right) + \frac{6m_W^4}{v^2} \left( \ln \frac{m_W^2}{Q^2} - \frac{1}{3} \right) \\ &\quad \left. + \frac{3m_Z^4}{v^2} \left( \ln \frac{m_Z^2}{Q^2} - \frac{1}{3} \right) - \frac{12m_t^4}{v^2} \left( \ln \frac{m_t^2}{Q^2} - 1 \right) \right] = 0, \end{aligned} \quad (\text{A2})$$

where

$$f_{\pm}(m_i^2, m_j^2) = m_i^2 \left( \ln \frac{m_i^2}{Q^2} - 1 \right) \pm m_j^2 \left( \ln \frac{m_j^2}{Q^2} - 1 \right), \quad (\text{A3})$$

$$\Delta m_{\Phi}^2 = m_{\Phi_2}^2 - m_{\Phi_1}^2 = \sqrt{(\mathcal{M}_{\Phi_1\Phi_1}^2 - \mathcal{M}_{\Phi_2\Phi_2}^2)^2 + 4\mathcal{M}_{\Phi_1\Phi_2}^4}, \quad (\text{A4})$$

$$\mathcal{M}_{neutral\ Higgs}^2 = \begin{pmatrix} \mathcal{M}_{\Phi_1\Phi_1}^2 & \mathcal{M}_{\Phi_1\Phi_2}^2 \\ \mathcal{M}_{\Phi_2\Phi_1}^2 & \mathcal{M}_{\Phi_2\Phi_2}^2 \end{pmatrix} \quad (\text{A5})$$

and the masses in the tadpole conditions of red point case are

$$m_{\Phi_{1,r}}^2 = -\mu_1^2 + 3\lambda_1 v^2, \quad m_{\Phi_{2,r}}^2 = -\mu_2^2 + \lambda_{12} v^2/2, \quad (\text{A6})$$

$$m_{N_{1,r}}^2 = -\mu_1^2 + \lambda_1 v^2, \quad m_{N_{2,r}}^2 = -\mu_2^2 + \lambda_{12} v^2/2, \quad (\text{A7})$$

with  $m_{\Phi_2}^2 > m_h^2$ . In order to replace two of the input parameters in the potential in terms of the Higgs boson

mass  $m_h$  and additional neutral CP-even boson mass  $m_{\Phi_2}$ <sup>1</sup>, we use

$$\left. \frac{\partial^2 V_{\text{eff}}}{\partial \langle \Phi_1 \rangle^2} \right|_{\langle \Phi_1 \rangle=v, \langle \Phi_2 \rangle=0} = 2\lambda_1 v^2 + \frac{v^2}{32\pi^2} \left[ A_2^r \ln \frac{m_{\Phi_2}^2 m_h^2}{Q^4} - A_3^r \ln \frac{m_h^2}{m_{\Phi_2}^2} + 4\lambda_{12}^2 (2(2I_{\Phi_2} - 1) - 1) \ln \frac{m_{N_{2,r}}^2}{Q^2} \right. \\ \left. + 12 \frac{m_Z^4}{v^4} \left( \ln \frac{m_Z^2}{Q^2} + \frac{2}{3} \right) + 24 \frac{m_W^4}{v^4} \left( \ln \frac{m_W^2}{Q^2} + \frac{2}{3} \right) - 48 \frac{m_t^4}{v^4} \ln \frac{m_t^2}{Q^2} \right] \equiv m_h^2 \quad (\text{A8})$$

$$\left. \frac{\partial^2 V_{\text{eff}}}{\partial \langle \Phi_2 \rangle^2} \right|_{\langle \Phi_1 \rangle=v, \langle \Phi_2 \rangle=0} = -\mu_2^2 + \lambda_{12} v^2 + \frac{1}{64\pi^2} \left[ B_1 f_-(m_{\Phi_2}^2, m_h^2) + B_2 f_+(m_{\Phi_2}^2, m_h^2) \right. \\ \left. + 4(2(2I_{\Phi_2} - 1) - 1) \lambda_2 m_{N_{2,r}}^2 \left( \ln \frac{m_{N_{2,r}}^2}{Q^2} - 1 \right) + 12 \frac{m_Z^4 Y_{\Phi_2}^2}{v^2} \left( \ln \frac{m_Z^2}{Q^2} - \frac{1}{3} \right) \right. \\ \left. + 24 \frac{m_W^4 I_W^2}{v^2} \left( \ln \frac{m_W^2}{Q^2} - \frac{1}{3} \right) \right] \equiv m_{\Phi_2}^2, \quad (\text{A9})$$

where

$$A_2^r = \frac{1}{4} \left( (6\lambda_1 + \lambda_{12})^2 + (6\lambda_1 - \lambda_{12})^2 \right), \quad (\text{A10})$$

$$A_3^r = -\frac{36\lambda_1^2 - \lambda_{12}^2}{2} \quad (\text{A11})$$

$$B_1 = \frac{2}{\Delta m^2} \left[ (-6\lambda_2 + \lambda_{12}) (\mathcal{M}_{\Phi_1 \Phi_1}^2 - \mathcal{M}_{\Phi_2 \Phi_2}^2) + 4\lambda_{12}^2 v^2 \right] \quad (\text{A12})$$

$$B_2 = 6\lambda_2 + \lambda_{12}. \quad (\text{A13})$$

By using Eqs. (A2), (A8) and (A9), we can replace the model parameters:

$$(\mu_1^2, \mu_2^2, \lambda_1, \lambda_2, \lambda_{12}) \rightarrow (v, m_{\Phi_2}^2, m_h, \lambda_2, \lambda_{12}). \quad (\text{A14})$$

## Appendix B: Landau pole in the model with CSI

In this section, we show the Landau pole in the model with CSI. The model with CSI typically has the large values of couplings, which can be obtained by Eq. (29). The results of the Landau pole is given by Fig. 14 According to Figs. 5 and 14, the parameter region with detectable GW spectrum has Landau pole, which is O(1 TeV). When the value of  $\lambda_2$  will be large, the Landau pole also will be small.

- [1] P.A. Zyla et al. (Particle Data Group), “Review of Particle Physics,” PTEP **2020**, 083C01 (2020).
- [2] Anupam Mazumdar and Graham White, “Review of cosmic phase transitions: their significance and experimental signatures,” Rept. Prog. Phys. **82**, 076901 (2019), arXiv:1811.01948 [hep-ph].
- [3] Mark B. Hindmarsh, Marvin Lüben, Johannes Lumma, and Martin Pauly, “Phase transitions in the early universe,” SciPost Phys. Lect. Notes **24**, 1 (2021), arXiv:2008.09136 [astro-ph.CO].
- [4] Chiara Caprini et al., “Science with the space-based interferometer eLISA. II: Gravitational waves from cos-

mological phase transitions,” JCAP **1604**, 001 (2016), arXiv:1512.06239 [astro-ph.CO].

- [5] Chiara Caprini et al., “Detecting gravitational waves from cosmological phase transitions with LISA: an update,” JCAP **2003**, 024 (2020), arXiv:1910.13125 [astro-ph.CO].
- [6] Pau Amaro-Seoane et al. (LISA), “Laser Interferometer Space Antenna,” (2017), arXiv:1702.00786 [astro-ph.IM].
- [7] Pierre Binétruy, Alejandro Bohe, Chiara Caprini, and Jean-Francois Dufaux, “Cosmological Backgrounds of Gravitational Waves and eLISA/NGO: Phase Transitions, Cosmic Strings and Other Sources,” JCAP **1206**, 027 (2012), arXiv:1201.0983 [gr-qc].
- [8] Pau Amaro-Seoane et al., “Low-frequency gravitational-wave science with eLISA/NGO,” Class. Quant. Grav. **29**, 124016 (2012), arXiv:1202.0839 [gr-qc].

<sup>1</sup> For simplicity, we ignore the contribution from the two-point-function  $\Pi_{hh}$  of the Higgs boson.

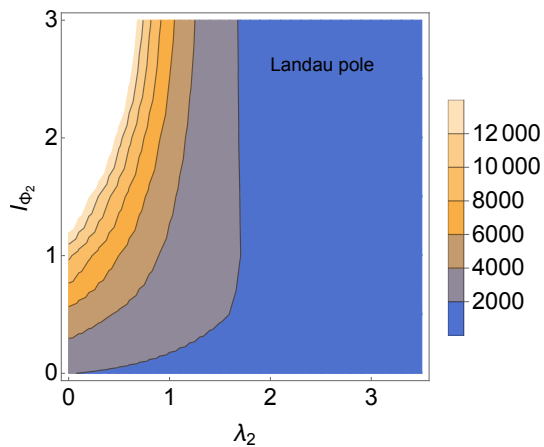


FIG. 14. The values of Landau pole in the CSI model.

- [9] Pau Amaro-Seoane *et al.*, “eLISA/NGO: Astrophysics and cosmology in the gravitational-wave millihertz regime,” *GW Notes* **6**, 4–110 (2013), arXiv:1201.3621 [astro-ph.CO].
- [10] David J. Weir, “Gravitational waves from a first order electroweak phase transition: a brief review,” *Phil. Trans. Roy. Soc. Lond.* **A376**, 20170126 (2018), arXiv:1705.01783 [hep-ph].
- [11] Daniel G. Figueroa, Eugenio Megias, Germano Nardini, Mauro Pieroni, Mariano Quiros, Angelo Ricciardone, and Gianmassimo Tassinato, “LISA as a probe for particle physics: electroweak scale tests in synergy with ground-based experiments,” *PoS GRASS2018*, 036 (2018), arXiv:1806.06463 [astro-ph.CO].
- [12] Margot Fitz Axen, Sharan Banagiri, Andrew Matas, Chiara Caprini, and Vuk Mandic, “Multiwavelength observations of cosmological phase transitions using LISA and Cosmic Explorer,” *Phys. Rev.* **D98**, 103508 (2018), arXiv:1806.02500 [astro-ph.IM].
- [13] Rong-Gen Cai, Zhoujian Cao, Zong-Kuan Guo, Shao-Jiang Wang, and Tao Yang, “The Gravitational-Wave Physics,” *Natl. Sci. Rev.* **4**, 687–706 (2017), arXiv:1703.00187 [gr-qc].
- [14] Ligong Bian *et al.*, “The Gravitational-wave physics II: Progress,” *Sci. China Phys. Mech. Astron.* **64**, 120401 (2021), arXiv:2106.10235 [gr-qc].
- [15] K. Kajantie, M. Laine, K. Rummukainen, and Mikhail E. Shaposhnikov, “Is there a hot electroweak phase transition at  $m(H)$  larger or equal to  $m(W)$ ?” *Phys. Rev. Lett.* **77**, 2887–2890 (1996), arXiv:hep-ph/9605288 [hep-ph].
- [16] Xin-min Zhang, “Operators analysis for Higgs potential and cosmological bound on Higgs mass,” *Phys. Rev.* **D47**, 3065–3067 (1993), arXiv:hep-ph/9301277 [hep-ph].
- [17] Dietrich Bodeker, Lars Fromme, Stephan J. Huber, and Michael Seniuch, “The Baryon asymmetry in the standard model with a low cut-off,” *JHEP* **02**, 026 (2005), arXiv:hep-ph/0412366 [hep-ph].
- [18] Christophe Grojean, Geraldine Servant, and James D. Wells, “First-order electroweak phase transition in the standard model with a low cutoff,” *Phys. Rev.* **D71**, 036001 (2005), arXiv:hep-ph/0407019 [hep-ph].
- [19] Cedric Delaunay, Christophe Grojean, and James D. Wells, “Dynamics of Non-renormalizable Electroweak Symmetry Breaking,” *JHEP* **04**, 029 (2008), arXiv:0711.2511 [hep-ph].
- [20] Stephan J. Huber and Thomas Konstandin, “Production of gravitational waves in the nMSSM,” *JCAP* **0805**, 017 (2008), arXiv:0709.2091 [hep-ph].
- [21] Stephan J. Huber and Miguel Sopena, “An efficient approach to electroweak bubble velocities,” (2013), arXiv:1302.1044 [hep-ph].
- [22] Thomas Konstandin, Germano Nardini, and Ingo Rues, “From Boltzmann equations to steady wall velocities,” *JCAP* **1409**, 028 (2014), arXiv:1407.3132 [hep-ph].
- [23] P. H. Damgaard, A. Haarr, D. O’Connell, and A. Tranberg, “Effective Field Theory and Electroweak Baryogenesis in the Singlet-Extended Standard Model,” *JHEP* **02**, 107 (2016), arXiv:1512.01963 [hep-ph].
- [24] Leonardo Leitao and Ariel Megevand, “Gravitational waves from a very strong electroweak phase transition,” *JCAP* **1605**, 037 (2016), arXiv:1512.08962 [astro-ph.CO].
- [25] Christopher P. D. Harman and Stephan J. Huber, “Does zero temperature decide on the nature of the electroweak phase transition?” *JHEP* **06**, 005 (2016), arXiv:1512.05611 [hep-ph].
- [26] Fa Peng Huang, Youping Wan, Dong-Gang Wang, Yi-Fu Cai, and Xinmin Zhang, “Hearing the echoes of electroweak baryogenesis with gravitational wave detectors,” *Phys. Rev.* **D94**, 041702 (2016), arXiv:1601.01640 [hep-ph].
- [27] Csaba Balazs, Graham White, and Jason Yue, “Effective field theory, electric dipole moments and electroweak baryogenesis,” *JHEP* **03**, 030 (2017), arXiv:1612.01270 [hep-ph].
- [28] Jordy de Vries, Marieke Postma, Jorinde van de Vis, and Graham White, “Electroweak Baryogenesis and the Standard Model Effective Field Theory,” *JHEP* **01**, 089 (2018), arXiv:1710.04061 [hep-ph].
- [29] Rong-Gen Cai, Misao Sasaki, and Shao-Jiang Wang, “The gravitational waves from the first-order phase transition with a dimension-six operator,” *JCAP* **1708**, 004 (2017), arXiv:1707.03001 [astro-ph.CO].
- [30] Mikael Chala, Claudius Krause, and Germano Nardini, “Signals of the electroweak phase transition at colliders and gravitational wave observatories,” *JHEP* **07**, 062 (2018), arXiv:1802.02168 [hep-ph].
- [31] Glauber C. Dorsch, Stephan J. Huber, and Thomas Konstandin, “Bubble wall velocities in the Standard Model and beyond,” *JCAP* **1812**, 034 (2018), arXiv:1809.04907 [hep-ph].
- [32] Jordy De Vries, Marieke Postma, and Jorinde van de Vis, “The role of leptons in electroweak baryogenesis,” *JHEP* **04**, 024 (2019), arXiv:1811.11104 [hep-ph].
- [33] Sebastian A. R. Ellis, Seyda Ipek, and Graham White, “Electroweak Baryogenesis from Temperature-Varying Couplings,” *JHEP* **08**, 002 (2019), arXiv:1905.11994 [hep-ph].
- [34] Mikael Chala, Valentin V. Khoze, Michael Spannowsky, and Philip Waite, “Mapping the shape of the scalar potential with gravitational waves,” *Int. J. Mod. Phys.* **A34**, 1950223 (2019), arXiv:1905.00911 [hep-ph].
- [35] Ruiyu Zhou, Ligong Bian, and Huai-Ke Guo, “Connecting the electroweak sphaleron with gravitational waves,”

- Phys. Rev. **D101**, 091903 (2020), arXiv:1910.00234 [hep-ph].
- [36] Vo Quoc Phong, Phan Hong Khiem, Ngo Phuc Duc Loc, and Hoang Ngoc Long, “Sphaleron in the first-order electroweak phase transition with the dimension-six Higgs field operator,” Phys. Rev. **D101**, 116010 (2020), arXiv:2003.09625 [hep-ph].
- [37] Shinya Kanemura and Masanori Tanaka, “Higgs boson coupling as a probe of the sphaleron property,” Phys. Lett. B **809**, 135711 (2020), arXiv:2005.05250 [hep-ph].
- [38] Katsuya Hashino, Shinya Kanemura, and Tomo Takahashi, “Primordial black holes as a probe of strongly first-order electroweak phase transition,” (2021), arXiv:2111.13099 [hep-ph].
- [39] Shinya Kanemura and Ryo Nagai, “A new Higgs effective field theory and the new no-lose theorem,” (2021), arXiv:2111.12585 [hep-ph].
- [40] Stefano Profumo, Michael J. Ramsey-Musolf, and Gabe Shaughnessy, “Singlet Higgs phenomenology and the electroweak phase transition,” JHEP **08**, 010 (2007), arXiv:0705.2425 [hep-ph].
- [41] Jose R. Espinosa, Thomas Konstandin, and Francesco Riva, “Strong Electroweak Phase Transitions in the Standard Model with a Singlet,” Nucl. Phys. **B854**, 592–630 (2012), arXiv:1107.5441 [hep-ph].
- [42] Stefano Profumo, Michael J. Ramsey-Musolf, Carroll L. Wainwright, and Peter Winslow, “Singlet-catalyzed electroweak phase transitions and precision Higgs boson studies,” Phys. Rev. **D91**, 035018 (2015), arXiv:1407.5342 [hep-ph].
- [43] Ryusuke Jinno, Kazunori Nakayama, and Masahiro Takimoto, “Gravitational waves from the first order phase transition of the Higgs field at high energy scales,” Phys. Rev. **D93**, 045024 (2016), arXiv:1510.02697 [hep-ph].
- [44] Peisi Huang, Andrew J. Long, and Lian-Tao Wang, “Probing the Electroweak Phase Transition with Higgs Factories and Gravitational Waves,” Phys. Rev. **D94**, 075008 (2016), arXiv:1608.06619 [hep-ph].
- [45] Csaba Balazs, Andrew Fowlie, Anupam Mazumdar, and Graham White, “Gravitational waves at aLIGO and vacuum stability with a scalar singlet extension of the Standard Model,” Phys. Rev. **D95**, 043505 (2017), arXiv:1611.01617 [hep-ph].
- [46] David Curtin, Patrick Meade, and Harikrishnan Raman, “Thermal Resummation and Phase Transitions,” Eur. Phys. J. **C78**, 787 (2018), arXiv:1612.00466 [hep-ph].
- [47] Katsuya Hashino, Mitsuru Kakizaki, Shinya Kanemura, Pyungwon Ko, and Toshinori Matsui, “Gravitational waves and Higgs boson couplings for exploring first order phase transition in the model with a singlet scalar field,” Phys. Lett. **B766**, 49–54 (2017), arXiv:1609.00297 [hep-ph].
- [48] Ville Vaskonen, “Electroweak baryogenesis and gravitational waves from a real scalar singlet,” Phys. Rev. **D95**, 123515 (2017), arXiv:1611.02073 [hep-ph].
- [49] Gowri Kurup and Maxim Perelstein, “Dynamics of Electroweak Phase Transition In Singlet-Scalar Extension of the Standard Model,” Phys. Rev. **D96**, 015036 (2017), arXiv:1704.03381 [hep-ph].
- [50] Ankit Beniwal, Marek Lewicki, James D. Wells, Martin White, and Anthony G. Williams, “Gravitational wave, collider and dark matter signals from a scalar singlet electroweak baryogenesis,” JHEP **08**, 108 (2017), arXiv:1702.06124 [hep-ph].
- [51] Zhaofeng Kang, P. Ko, and Toshinori Matsui, “Strong first order EWPT & strong gravitational waves in  $Z_3$ -symmetric singlet scalar extension,” JHEP **02**, 115 (2018), arXiv:1706.09721 [hep-ph].
- [52] Chien-Yi Chen, Jonathan Kozaczuk, and Ian M. Lewis, “Non-resonant Collider Signatures of a Singlet-Driven Electroweak Phase Transition,” JHEP **08**, 096 (2017), arXiv:1704.05844 [hep-ph].
- [53] Wei Chao, Huai-Ke Guo, and Jing Shu, “Gravitational Wave Signals of Electroweak Phase Transition Triggered by Dark Matter,” JCAP **1709**, 009 (2017), arXiv:1702.02698 [hep-ph].
- [54] Ankit Beniwal, Marek Lewicki, Martin White, and Anthony G. Williams, “Gravitational waves and electroweak baryogenesis in a global study of the extended scalar singlet model,” JHEP **02**, 183 (2019), arXiv:1810.02380 [hep-ph].
- [55] Vahid Reza Shajiee and Ali Tofighi, “Electroweak Phase Transition, Gravitational Waves and Dark Matter in Two Scalar Singlet Extension of The Standard Model,” Eur. Phys. J. **C79**, 360 (2019), arXiv:1811.09807 [hep-ph].
- [56] Alexandre Alves, Tathagata Ghosh, Huai-Ke Guo, Kuber Sinha, and Daniel Vagie, “Collider and Gravitational Wave Complementarity in Exploring the Singlet Extension of the Standard Model,” JHEP **04**, 052 (2019), arXiv:1812.09333 [hep-ph].
- [57] Bohdan Grzadkowski and Da Huang, “Spontaneous  $CP$ -Violating Electroweak Baryogenesis and Dark Matter from a Complex Singlet Scalar,” JHEP **08**, 135 (2018), arXiv:1807.06987 [hep-ph].
- [58] Katsuya Hashino, Ryusuke Jinno, Mitsuru Kakizaki, Shinya Kanemura, Tomo Takahashi, and Masahiro Takimoto, “Selecting models of first-order phase transitions using the synergy between collider and gravitational-wave experiments,” Phys. Rev. **D99**, 075011 (2019), arXiv:1809.04994 [hep-ph].
- [59] Amine Ahriche, Katsuya Hashino, Shinya Kanemura, and Salah Nasri, “Gravitational Waves from Phase Transitions in Models with Charged Singlets,” Phys. Lett. **B789**, 119–126 (2019), arXiv:1809.09883 [hep-ph].
- [60] Batool Imtiaz, Yi-Fu Cai, and Youping Wan, “Two-field cosmological phase transitions and gravitational waves in the singlet Majoron model,” Eur. Phys. J. **C79**, 25 (2019), arXiv:1804.05835 [hep-ph].
- [61] Ning Chen, Tong Li, Yongcheng Wu, and Ligong Bian, “Complementarity of the future  $e^+e^-$  colliders and gravitational waves in the probe of complex singlet extension to the standard model,” Phys. Rev. **D101**, 075047 (2020), arXiv:1911.05579 [hep-ph].
- [62] Alexandre Alves, Dorival Gonçalves, Tathagata Ghosh, Huai-Ke Guo, and Kuber Sinha, “Di-Higgs Production in the  $4b$  Channel and Gravitational Wave Complementarity,” JHEP **03**, 053 (2020), arXiv:1909.05268 [hep-ph].
- [63] Kristjan Kannike, Kaius Loos, and Martti Raidal, “Gravitational wave signals of pseudo-Goldstone dark matter in the  $Z_3$  complex singlet model,” Phys. Rev. **D101**, 035001 (2020), arXiv:1907.13136 [hep-ph].
- [64] Cheng-Wei Chiang and Bo-Qiang Lu, “First-order electroweak phase transition in a complex singlet model with  $Z_3$  symmetry,” JHEP **07**, 082 (2020),

- arXiv:1912.12634 [hep-ph].
- [65] Jonathan Kozaczuk, Michael J. Ramsey-Musolf, and Jessie Shelton, “Exotic Higgs boson decays and the electroweak phase transition,” *Phys. Rev.* **D101**, 115035 (2020), arXiv:1911.10210 [hep-ph].
- [66] Marcela Carena, Zhen Liu, and Yikun Wang, “Electroweak phase transition with spontaneous  $Z_2$ -breaking,” *JHEP* **08**, 107 (2020), arXiv:1911.10206 [hep-ph].
- [67] Alexandre Alves, Dorival Gonçalves, Tathagata Ghosh, Huai-Ke Guo, and Kuver Sinha, “Di-Higgs Blind Spots in Gravitational Wave Signals,” *Phys. Lett. B* **818**, 136377 (2021), arXiv:2007.15654 [hep-ph].
- [68] Pasquale Di Bari, Danny Marfatia, and Ye-Ling Zhou, “Gravitational waves from neutrino mass and dark matter genesis,” *Phys. Rev.* **D102**, 095017 (2020), arXiv:2001.07637 [hep-ph].
- [69] Madhurima Pandey and Avik Paul, “Gravitational Wave Emissions from First Order Phase Transitions with Two Component FIMP Dark Matter,” (2020), arXiv:2003.08828 [hep-ph].
- [70] Tommi Alanne, Nico Benincasa, Matti Heikinheimo, Kristjan Kannike, Venus Keus, Niko Koivunen, and Kimmo Tuominen, “Pseudo-Goldstone dark matter: gravitational waves and direct-detection blind spots,” *JHEP* **10**, 080 (2020), arXiv:2008.09605 [hep-ph].
- [71] Avik Paul, Upala Mukhopadhyay, and Debasish Majumdar, “Gravitational Wave Signatures from Domain Wall and Strong First-Order Phase Transitions in a Two Complex Scalar extension of the Standard Model,” *JHEP* **05**, 223 (2021), arXiv:2010.03439 [hep-ph].
- [72] Ke-Pan Xie, “Lepton-mediated electroweak baryogenesis, gravitational waves and the  $4\pi$  final state at the collider,” *JHEP* **02**, 090 (2021), arXiv:2011.04821 [hep-ph].
- [73] Shinya Kanemura and Masanori Tanaka, “Strongly first-order electroweak phase transition by relatively heavy additional Higgs bosons,” (2022), arXiv:2201.04791 [hep-ph].
- [74] Patrick Huet and Ann E. Nelson, “CP violation and electroweak baryogenesis in extensions of the standard model,” *Phys. Lett.* **B355**, 229–235 (1995), arXiv:hep-ph/9504427 [hep-ph].
- [75] James M. Cline and Pierre-Anthony Lemieux, “Electroweak phase transition in two Higgs doublet models,” *Phys. Rev.* **D55**, 3873–3881 (1997), arXiv:hep-ph/9609240 [hep-ph].
- [76] Lars Fromme, Stephan J. Huber, and Michael Seniuch, “Baryogenesis in the two-Higgs doublet model,” *JHEP* **11**, 038 (2006), arXiv:hep-ph/0605242 [hep-ph].
- [77] James M. Cline, Kimmo Kainulainen, and Michael Trott, “Electroweak Baryogenesis in Two Higgs Doublet Models and B meson anomalies,” *JHEP* **11**, 089 (2011), arXiv:1107.3559 [hep-ph].
- [78] G. C. Dorsch, S. J. Huber, and J. M. No, “A strong electroweak phase transition in the 2HDM after LHC8,” *JHEP* **10**, 029 (2013), arXiv:1305.6610 [hep-ph].
- [79] G. C. Dorsch, S. J. Huber, K. Mimasu, and J. M. No, “Echoes of the Electroweak Phase Transition: Discovering a second Higgs doublet through  $A_0 \rightarrow ZH_0$ ,” *Phys. Rev. Lett.* **113**, 211802 (2014), arXiv:1405.5537 [hep-ph].
- [80] Mitsuru Kakizaki, Shinya Kanemura, and Toshihiko Matsui, “Gravitational waves as a probe of extended scalar sectors with the first order electroweak phase transition,” *Phys. Rev.* **D92**, 115007 (2015), arXiv:1509.08394 [hep-ph].
- [81] G. C. Dorsch, S. J. Huber, T. Konstandin, and J. M. No, “A Second Higgs Doublet in the Early Universe: Baryogenesis and Gravitational Waves,” *JCAP* **1705**, 052 (2017), arXiv:1611.05874 [hep-ph].
- [82] P. Basler, M. Krause, M. Muhlleitner, J. Wittbrodt, and A. Wlotzka, “Strong First Order Electroweak Phase Transition in the CP-Conserving 2HDM Revisited,” *JHEP* **02**, 121 (2017), arXiv:1612.04086 [hep-ph].
- [83] Jérémy Bernon, Ligong Bian, and Yun Jiang, “A new insight into the phase transition in the early Universe with two Higgs doublets,” *JHEP* **05**, 151 (2018), arXiv:1712.08430 [hep-ph].
- [84] G. C. Dorsch, S. J. Huber, K. Mimasu, and J. M. No, “The Higgs Vacuum Uplifted: Revisiting the Electroweak Phase Transition with a Second Higgs Doublet,” *JHEP* **12**, 086 (2017), arXiv:1705.09186 [hep-ph].
- [85] Fa Peng Huang and Jiang-Hao Yu, “Exploring inert dark matter blind spots with gravitational wave signatures,” *Phys. Rev.* **D98**, 095022 (2018), arXiv:1704.04201 [hep-ph].
- [86] Philipp Basler, Margarete Mühlleitner, and Jonas Wittbrodt, “The CP-Violating 2HDM in Light of a Strong First Order Electroweak Phase Transition and Implications for Higgs Pair Production,” *JHEP* **03**, 061 (2018), arXiv:1711.04097 [hep-ph].
- [87] Basabendu Barman, Amit Dutta Banik, and Avik Paul, “Singlet-doublet fermionic dark matter and gravitational waves in a two-Higgs-doublet extension of the Standard Model,” *Phys. Rev.* **D101**, 055028 (2020), arXiv:1912.12899 [hep-ph].
- [88] Xiao Wang, Fa Peng Huang, and Xinmin Zhang, “Gravitational wave and collider signals in complex two-Higgs doublet model with dynamical CP-violation at finite temperature,” *Phys. Rev.* **D101**, 015015 (2020), arXiv:1909.02978 [hep-ph].
- [89] Ruiyu Zhou and Ligong Bian, “Baryon asymmetry and detectable Gravitational Waves from Electroweak phase transition,” (2020), arXiv:2001.01237 [hep-ph].
- [90] Dorival Gonçalves, Ajay Kaladharan, and Yongcheng Wu, “Electroweak phase transition in the 2HDM: collider and gravitational wave complementarity,” (2021), arXiv:2108.05356 [hep-ph].
- [91] Lukáš Gráf, Sudip Jana, Ajay Kaladharan, and Shaikh Saad, “Gravitational Wave Imprints of Left-Right Symmetric Model with Minimal Higgs Sector,” (2021), arXiv:2112.12041 [hep-ph].
- [92] Hiren H. Patel and Michael J. Ramsey-Musolf, “Stepping Into Electroweak Symmetry Breaking: Phase Transitions and Higgs Phenomenology,” *Phys. Rev.* **D88**, 035013 (2013), arXiv:1212.5652 [hep-ph].
- [93] Satoru Inoue, Grigory Ovanesyan, and Michael J. Ramsey-Musolf, “Two-Step Electroweak Baryogenesis,” *Phys. Rev.* **D93**, 015013 (2016), arXiv:1508.05404 [hep-ph].
- [94] Nikita Blinov, Jonathan Kozaczuk, David E. Morrissey, and Carlos Tamarit, “Electroweak Baryogenesis from Exotic Electroweak Symmetry Breaking,” *Phys. Rev.* **D92**, 035012 (2015), arXiv:1504.05195 [hep-ph].
- [95] Mikael Chala, Maria Ramos, and Michael Spannowsky, “Gravitational wave and collider probes of a triplet Higgs sector with a low cutoff,” *Eur. Phys. J.* **C79**, 156

- (2019), arXiv:1812.01901 [hep-ph].
- [96] Ruiyu Zhou, Wei Cheng, Xin Deng, Ligong Bian, and Yongcheng Wu, “Electroweak phase transition and Higgs phenomenology in the Georgi-Machacek model,” *JHEP* **01**, 216 (2019), arXiv:1812.06217 [hep-ph].
- [97] Andrea Addazi, Antonino Marcianò, António P. Morais, Roman Pasechnik, Rahul Srivastava, and José W. F. Valle, “Gravitational footprints of massive neutrinos and lepton number breaking,” *Phys. Lett.* **B807**, 135577 (2020), arXiv:1909.09740 [hep-ph].
- [98] Nico Benincasa, Kristjan Kannike, Andi Hektor, Andrzej Hryczuk, and Kaius Loos, “Phase transitions and gravitational waves in models of  $\mathbb{Z}_N$  scalar dark matter,” *Proceedings, 2019 European Physical Society Conference on High Energy Physics (EPS-HEP2019): Ghent, Belgium, PoS EPS-HEP2019*, 089 (2020).
- [99] Vedran Brdar, Lukas Graf, Alexander J. Helmboldt, and Xun-Jie Xu, “Gravitational Waves as a Probe of Left-Right Symmetry Breaking,” *JCAP* **1912**, 027 (2019), arXiv:1909.02018 [hep-ph].
- [100] Avik Paul, Biswajit Banerjee, and Debasish Majumdar, “Gravitational wave signatures from an extended inert doublet dark matter model,” *JCAP* **1910**, 062 (2019), arXiv:1908.00829 [hep-ph].
- [101] Ligong Bian, Huai-Ke Guo, Yongcheng Wu, and Ruiyu Zhou, “Gravitational wave and collider searches for electroweak symmetry breaking patterns,” *Phys. Rev.* **D101**, 035011 (2020), arXiv:1906.11664 [hep-ph].
- [102] Lauri Niemi, Michael J. Ramsey-Musolf, Tuomas V. I. Tenkanen, and David J. Weir, “Thermodynamics of a Two-Step Electroweak Phase Transition,” *Phys. Rev. Lett.* **126**, 171802 (2021), arXiv:2005.11332 [hep-ph].
- [103] Yan Wang, Chong Sheng Li, and Fa Peng Huang, “Complementary probe of dark matter blind spots by lepton colliders and gravitational waves,” *Phys. Rev. D* **104**, 053004 (2021), arXiv:2012.03920 [hep-ph].
- [104] Debasish Borah, Arnab Dasgupta, Kohei Fujikura, Sin Kyu Kang, and Devabrat Mahanta, “Observable Gravitational Waves in Minimal Scotogenic Model,” *JCAP* **2008**, 046 (2020), arXiv:2003.02276 [hep-ph].
- [105] Benjamin Grinstein and Michael Trott, “Electroweak Baryogenesis with a Pseudo-Goldstone Higgs,” *Phys. Rev.* **D78**, 075022 (2008), arXiv:0806.1971 [hep-ph].
- [106] Giuliano Panico, Michele Redi, Andrea Tesi, and Andrea Wulzer, “On the Tuning and the Mass of the Composite Higgs,” *JHEP* **03**, 051 (2013), arXiv:1210.7114 [hep-ph].
- [107] Christophe Grojean, Oleksii Matsedonskyi, and Giuliano Panico, “Light top partners and precision physics,” *JHEP* **10**, 160 (2013), arXiv:1306.4655 [hep-ph].
- [108] Csaba Csáki, Michael Geller, and Ofri Telem, “Tree-level Quartic for a Holographic Composite Higgs,” *JHEP* **05**, 134 (2018), arXiv:1710.08921 [hep-ph].
- [109] Jose R. Espinosa, Ben Gripaios, Thomas Konstandin, and Francesco Riva, “Electroweak Baryogenesis in Non-minimal Composite Higgs Models,” *JCAP* **1201**, 012 (2012), arXiv:1110.2876 [hep-ph].
- [110] Ligong Bian, Yongcheng Wu, and Ke-Pan Xie, “Electroweak phase transition with composite Higgs models: calculability, gravitational waves and collider searches,” *JHEP* **12**, 028 (2019), arXiv:1909.02014 [hep-ph].
- [111] Stefania De Curtis, Luigi Delle Rose, and Giuliano Panico, “Composite Dynamics in the Early Universe,” *JHEP* **12**, 149 (2019), arXiv:1909.07894 [hep-ph].
- [112] Ke-Pan Xie, Ligong Bian, and Yongcheng Wu, “Electroweak baryogenesis and gravitational waves in a composite Higgs model with high dimensional fermion representations,” *JHEP* **12**, 047 (2020), arXiv:2005.13552 [hep-ph].
- [113] Mikael Chala, Germano Nardini, and Ivan Sobolev, “Unified explanation for dark matter and electroweak baryogenesis with direct detection and gravitational wave signatures,” *Phys. Rev.* **D94**, 055006 (2016), arXiv:1605.08663 [hep-ph].
- [114] Kohei Fujikura, Kohei Kamada, Yuichiro Nakai, and Masahide Yamaguchi, “Phase Transitions in Twin Higgs Models,” *JHEP* **12**, 018 (2018), arXiv:1810.00574 [hep-ph].
- [115] Mikael Chala, Ramona Gröber, and Michael Spannowsky, “Searches for vector-like quarks at future colliders and implications for composite Higgs models with dark matter,” *JHEP* **03**, 040 (2018), arXiv:1801.06537 [hep-ph].
- [116] Sebastian Bruggisser, Benedict Von Harling, Oleksii Matsedonskyi, and Géraldine Servant, “Electroweak Phase Transition and Baryogenesis in Composite Higgs Models,” *JHEP* **12**, 099 (2018), arXiv:1804.07314 [hep-ph].
- [117] Sebastian Bruggisser, Benedict Von Harling, Oleksii Matsedonskyi, and Géraldine Servant, “Baryon Asymmetry from a Composite Higgs Boson,” *Phys. Rev. Lett.* **121**, 131801 (2018), arXiv:1803.08546 [hep-ph].
- [118] D. Delepine, J. M. Gerard, R. Gonzalez Felipe, and J. Weyers, “A Light stop and electroweak baryogenesis,” *Phys. Lett.* **B386**, 183–188 (1996), arXiv:hep-ph/9604440 [hep-ph].
- [119] Marcela Carena, M. Quiros, and C. E. M. Wagner, “Opening the window for electroweak baryogenesis,” *Phys. Lett.* **B380**, 81–91 (1996), arXiv:hep-ph/9603420 [hep-ph].
- [120] Riccardo Apreda, Michele Maggiore, Alberto Nicolis, and Antonio Riotto, “Supersymmetric phase transitions and gravitational waves at LISA,” *Class. Quant. Grav.* **18**, L155–L162 (2001), arXiv:hep-ph/0102140 [hep-ph].
- [121] M. Laine, G. Nardini, and K. Rummukainen, “Lattice study of an electroweak phase transition at  $m_h \simeq 126$  GeV,” *JCAP* **1301**, 011 (2013), arXiv:1211.7344 [hep-ph].
- [122] Leonardo Leitao, Ariel Megevand, and Alejandro D. Sanchez, “Gravitational waves from the electroweak phase transition,” *JCAP* **1210**, 024 (2012), arXiv:1205.3070 [astro-ph.CO].
- [123] Arjun Menon and David E. Morrissey, “Higgs Boson Signatures of MSSM Electroweak Baryogenesis,” *Phys. Rev.* **D79**, 115020 (2009), arXiv:0903.3038 [hep-ph].
- [124] David Curtin, Prerit Jaiswal, and Patrick Meade, “Excluding Electroweak Baryogenesis in the MSSM,” *JHEP* **08**, 005 (2012), arXiv:1203.2932 [hep-ph].
- [125] Marcela Carena, Germano Nardini, Mariano Quiros, and Carlos E. M. Wagner, “MSSM Electroweak Baryogenesis and LHC Data,” *JHEP* **02**, 001 (2013), arXiv:1207.6330 [hep-ph].
- [126] Timothy Cohen, David E. Morrissey, and Aaron Pierce, “Electroweak Baryogenesis and Higgs Signatures,” *Phys. Rev.* **D86**, 013009 (2012), arXiv:1203.2924 [hep-ph].
- [127] Stefan Liebler, Stefano Profumo, and Tim Stefaniak, “Light Stop Mass Limits from Higgs Rate Measure-

- ments in the MSSM: Is MSSM Electroweak Baryogenesis Still Alive After All?” *JHEP* **04**, 143 (2016), arXiv:1512.09172 [hep-ph].
- [128] Andrey Katz, Maxim Perelstein, Michael J. Ramsey-Musolf, and Peter Winslow, “Stop-Catalyzed Baryogenesis Beyond the MSSM,” *Phys. Rev.* **D92**, 095019 (2015), arXiv:1509.02934 [hep-ph].
- [129] Massimo Pietroni, “The Electroweak phase transition in a nonminimal supersymmetric model,” *Nucl. Phys.* **B402**, 27–45 (1993), arXiv:hep-ph/9207227 [hep-ph].
- [130] A. T. Davies, C. D. Froggatt, and R. G. Moorhouse, “Electroweak baryogenesis in the next-to-minimal supersymmetric model,” *Phys. Lett.* **B372**, 88–94 (1996), arXiv:hep-ph/9603388 [hep-ph].
- [131] Riccardo Apreda, Michele Maggiore, Alberto Nicolis, and Antonio Riotto, “Gravitational waves from electroweak phase transitions,” *Nucl. Phys.* **B631**, 342–368 (2002), arXiv:gr-qc/0107033 [gr-qc].
- [132] A. Menon, D. E. Morrissey, and C. E. M. Wagner, “Electroweak baryogenesis and dark matter in the nMSSM,” *Phys. Rev.* **D70**, 035005 (2004), arXiv:hep-ph/0404184 [hep-ph].
- [133] Subinoy Das, Patrick J. Fox, Abhishek Kumar, and Neal Weiner, “The Dark Side of the Electroweak Phase Transition,” *JHEP* **11**, 108 (2010), arXiv:0910.1262 [hep-ph].
- [134] Jonathan Kozaczuk, Stefano Profumo, and Carroll L. Wainwright, “Electroweak Baryogenesis And The Fermi Gamma-Ray Line,” *Phys. Rev.* **D87**, 075011 (2013), arXiv:1302.4781 [hep-ph].
- [135] Jonathan Kozaczuk, Stefano Profumo, Laurel Stephenson Haskins, and Carroll L. Wainwright, “Cosmological Phase Transitions and their Properties in the NMSSM,” *JHEP* **01**, 144 (2015), arXiv:1407.4134 [hep-ph].
- [136] Stephan J. Huber, Thomas Konstandin, Germano Nardini, and Ingo Rues, “Detectable Gravitational Waves from Very Strong Phase Transitions in the General NMSSM,” *JCAP* **1603**, 036 (2016), arXiv:1512.06357 [hep-ph].
- [137] S. V. Demidov, D. S. Gorbunov, and D. V. Kirpichnikov, “Split NMSSM with electroweak baryogenesis,” *JHEP* **11**, 148 (2016), [Erratum: *JHEP*08,080(2017)], arXiv:1608.01985 [hep-ph].
- [138] S. V. Demidov, D. S. Gorbunov, and D. V. Kirpichnikov, “Gravitational waves from phase transition in split NMSSM,” *Phys. Lett.* **B779**, 191–194 (2018), arXiv:1712.00087 [hep-ph].
- [139] Ligong Bian, Huai-Ke Guo, and Jing Shu, “Gravitational Waves, baryon asymmetry of the universe and electric dipole moment in the CP-violating NMSSM,” *Chin. Phys.* **C42**, 093106 (2018), [Erratum: *Chin. Phys.*C43,no.12,129101(2019)], arXiv:1704.02488 [hep-ph].
- [140] Sujeet Akula, Csaba Balázs, Liam Dunn, and Graham White, “Electroweak baryogenesis in the  $Z_3$ -invariant NMSSM,” *JHEP* **11**, 051 (2017), arXiv:1706.09898 [hep-ph].
- [141] Howard Georgi and Marie Machacek, “DOUBLY CHARGED HIGGS BOSONS,” *Nucl. Phys.* **B262**, 463–477 (1985).
- [142] Luis Cort, Mateo Garcia, and Mariano Quiros, “Supersymmetric Custodial Triplets,” *Phys. Rev.* **D88**, 075010 (2013), arXiv:1308.4025 [hep-ph].
- [143] Mateo Garcia-Pepin and Mariano Quiros, “Strong electroweak phase transition from Supersymmetric Custodial Triplets,” *JHEP* **05**, 177 (2016), arXiv:1602.01351 [hep-ph].
- [144] Roberto Vega, Roberto Vega-Morales, and Keping Xie, “The Supersymmetric Georgi-Machacek Model,” *JHEP* **03**, 168 (2018), arXiv:1711.05329 [hep-ph].
- [145] Paolo Creminelli, Alberto Nicolis, and Riccardo Rattazzi, “Holography and the electroweak phase transition,” *JHEP* **03**, 051 (2002), arXiv:hep-th/0107141 [hep-th].
- [146] Lisa Randall and Geraldine Servant, “Gravitational waves from warped spacetime,” *JHEP* **05**, 054 (2007), arXiv:hep-ph/0607158 [hep-ph].
- [147] Babiker Hassanain, John March-Russell, and Martin Schvellinger, “Warped Deformed Throats have Faster (Electroweak) Phase Transitions,” *JHEP* **10**, 089 (2007), arXiv:0708.2060 [hep-th].
- [148] Germano Nardini, Mariano Quiros, and Andrea Wulzer, “A Confining Strong First-Order Electroweak Phase Transition,” *JHEP* **09**, 077 (2007), arXiv:0706.3388 [hep-ph].
- [149] Thomas Konstandin, Germano Nardini, and Mariano Quiros, “Gravitational Backreaction Effects on the Holographic Phase Transition,” *Phys. Rev.* **D82**, 083513 (2010), arXiv:1007.1468 [hep-ph].
- [150] Thomas Konstandin and Geraldine Servant, “Cosmological Consequences of Nearly Conformal Dynamics at the TeV scale,” *JCAP* **1112**, 009 (2011), arXiv:1104.4791 [hep-ph].
- [151] Geraldine Servant, “Baryogenesis from Strong  $CP$  Violation and the QCD Axion,” *Phys. Rev. Lett.* **113**, 171803 (2014), arXiv:1407.0030 [hep-ph].
- [152] Yidian Chen, Mei Huang, and Qi-Shu Yan, “Gravitational waves from QCD and electroweak phase transitions,” *JHEP* **05**, 178 (2018), arXiv:1712.03470 [hep-ph].
- [153] Barry M. Dillon, Basem Kamal El-Menoufi, Stephan J. Huber, and Jonathan P. Manuel, “Rapid holographic phase transition with brane-localized curvature,” *Phys. Rev.* **D98**, 086005 (2018), arXiv:1708.02953 [hep-th].
- [154] Don Bunk, Jay Hubisz, and Bithika Jain, “A Perturbative RS I Cosmological Phase Transition,” *Eur. Phys. J.* **C78**, 78 (2018), arXiv:1705.00001 [hep-ph].
- [155] Luca Marzola, Antonio Racioppi, and Ville Vaskonen, “Phase transition and gravitational wave phenomenology of scalar conformal extensions of the Standard Model,” *Eur. Phys. J.* **C77**, 484 (2017), arXiv:1704.01034 [hep-ph].
- [156] Satoshi Iso, Pasquale D. Serpico, and Kengo Shimada, “QCD-Electroweak First-Order Phase Transition in a Supercooled Universe,” *Phys. Rev. Lett.* **119**, 141301 (2017), arXiv:1704.04955 [hep-ph].
- [157] Benedict von Harling and Geraldine Servant, “QCD-induced Electroweak Phase Transition,” *JHEP* **01**, 159 (2018), arXiv:1711.11554 [hep-ph].
- [158] Eugenio Megias, Germano Nardini, and Mariano Quiros, “Cosmological Phase Transitions in Warped Space: Gravitational Waves and Collider Signatures,” *JHEP* **09**, 095 (2018), arXiv:1806.04877 [hep-ph].
- [159] Kohei Fujikura, Yuichiro Nakai, and Masaki Yamada, “A more attractive scheme for radion stabilization and supercooled phase transition,” *JHEP* **02**, 111 (2020), arXiv:1910.07546 [hep-ph].

- [160] Kaustubh Agashe, Peizhi Du, Majid Ekhterachian, Soubhik Kumar, and Raman Sundrum, “Phase Transitions from the Fifth Dimension,” *JHEP* **02**, 051 (2021), arXiv:2010.04083 [hep-th].
- [161] Aleksandr Azatov and Miguel Vanvlasselaer, “Phase transitions in perturbative walking dynamics,” *JHEP* **09**, 085 (2020), arXiv:2003.10265 [hep-ph].
- [162] Francesco Bigazzi, Alessio Caddeo, Aldo L. Cotrone, and Angel Paredes, “Fate of false vacua in holographic first-order phase transitions,” *JHEP* **12**, 200 (2020), arXiv:2008.02579 [hep-th].
- [163] Eugenio Megias, Germano Nardini, and Mariano Quiros, “Gravitational Imprints from Heavy Kaluza-Klein Resonances,” *Phys. Rev.* **D102**, 055004 (2020), arXiv:2005.04127 [hep-ph].
- [164] J. R. Espinosa, T. Konstandin, J. M. No, and M. Quiros, “Some Cosmological Implications of Hidden Sectors,” *Phys. Rev.* **D78**, 123528 (2008), arXiv:0809.3215 [hep-ph].
- [165] Satoshi Iso, Nobuchika Okada, and Yuta Orikasa, “Classically conformal  $B-L$  extended Standard Model,” *Phys. Lett.* **B676**, 81–87 (2009), arXiv:0902.4050 [hep-ph].
- [166] Satoshi Iso, Nobuchika Okada, and Yuta Orikasa, “The minimal B-L model naturally realized at TeV scale,” *Phys. Rev.* **D80**, 115007 (2009), arXiv:0909.0128 [hep-ph].
- [167] Hiroshi Okada and Yuta Orikasa, “Classically conformal radiative neutrino model with gauged B-L symmetry,” *Phys. Lett.* **B760**, 558–564 (2016), arXiv:1412.3616 [hep-ph].
- [168] Glauber C. Dorsch, Stephan J. Huber, and Jose Miguel No, “Cosmological Signatures of a UV-Conformal Standard Model,” *Phys. Rev. Lett.* **113**, 121801 (2014), arXiv:1403.5583 [hep-ph].
- [169] Arsham Farzinnia and Jing Ren, “Higgs Partner Searches and Dark Matter Phenomenology in a Classically Scale Invariant Higgs Boson Sector,” *Phys. Rev.* **D90**, 015019 (2014), arXiv:1405.0498 [hep-ph].
- [170] Arsham Farzinnia and Jing Ren, “Strongly First-Order Electroweak Phase Transition and Classical Scale Invariance,” *Phys. Rev.* **D90**, 075012 (2014), arXiv:1408.3533 [hep-ph].
- [171] Joerg Jaeckel, Valentin V. Khoze, and Michael Spannowsky, “Hearing the signal of dark sectors with gravitational wave detectors,” *Phys. Rev.* **D94**, 103519 (2016), arXiv:1602.03901 [hep-ph].
- [172] Katsuya Hashino, Mitsuru Kakizaki, Shinya Kanemura, and Toshinori Matsui, “Synergy between measurements of gravitational waves and the triple-Higgs coupling in probing the first-order electroweak phase transition,” *Phys. Rev.* **D94**, 015005 (2016), arXiv:1604.02069 [hep-ph].
- [173] Ryusuke Jinno and Masahiro Takimoto, “Probing a classically conformal B-L model with gravitational waves,” *Phys. Rev.* **D95**, 015020 (2017), arXiv:1604.05035 [hep-ph].
- [174] Jisuke Kubo and Masatoshi Yamada, “Scale genesis and gravitational wave in a classically scale invariant extension of the standard model,” *JCAP* **1612**, 001 (2016), arXiv:1610.02241 [hep-ph].
- [175] Cheng-Wei Chiang and Eibun Senaha, “On gauge dependence of gravitational waves from a first-order phase transition in classical scale-invariant  $U(1)'$  models,” *Phys. Lett.* **B774**, 489–493 (2017), arXiv:1707.06765 [hep-ph].
- [176] Kohtaroh Miura, Hiroshi Ohki, Saeko Otani, and Koichi Yamawaki, “Gravitational Waves from Walking Technicolor,” *JHEP* **10**, 194 (2019), arXiv:1811.05670 [hep-ph].
- [177] Vedran Brdar, Alexander J. Helmboldt, and Jisuke Kubo, “Gravitational Waves from First-Order Phase Transitions: LIGO as a Window to Unexplored Seesaw Scales,” *JCAP* **1902**, 021 (2019), arXiv:1810.12306 [hep-ph].
- [178] Carlo Marzo, Luca Marzola, and Ville Vaskonen, “Phase transition and vacuum stability in the classically conformal B-L model,” *Eur. Phys. J.* **C79**, 601 (2019), arXiv:1811.11169 [hep-ph].
- [179] Tomislav Prokopec, Jonas Rezacek, and Bogumiła Świeżewska, “Gravitational waves from conformal symmetry breaking,” *JCAP* **1902**, 009 (2019), arXiv:1809.11129 [hep-ph].
- [180] Mayumi Aoki and Jisuke Kubo, “Gravitational waves from chiral phase transition in a conformally extended standard model,” *JCAP* **2004**, 001 (2020), arXiv:1910.05025 [hep-ph].
- [181] Ligong Bian, Wei Cheng, Huai-Ke Guo, and Yongchao Zhang, “Cosmological implications of a B – L charged hidden scalar: leptogenesis and gravitational waves,” *Chin. Phys. C* **45**, 113104 (2021), arXiv:1907.13589 [hep-ph].
- [182] Ahmad Mohamadnejad, “Gravitational waves from scale-invariant vector dark matter model: Probing below the neutrino-floor,” *Eur. Phys. J.* **C80**, 197 (2020), arXiv:1907.08899 [hep-ph].
- [183] Zhaofeng Kang and Jiang Zhu, “Scale-genesis by Dark Matter and Its Gravitational Wave Signal,” *Phys. Rev.* **D102**, 053011 (2020), arXiv:2003.02465 [hep-ph].
- [184] F. A. Chishtie, Zhuo-Ran Huang, M. Reimer, T. G. Steele, and Zhi-Wei Wang, “Transformation of scalar couplings between Coleman-Weinberg and MS schemes,” *Phys. Rev.* **D102**, 076021 (2020), arXiv:2003.01657 [hep-ph].
- [185] Pedro Schwaller, Tim M. P. Tait, and Roberto Vega-Morales, “Dark Matter and Vectorlike Leptons from Gauged Lepton Number,” *Phys. Rev.* **D88**, 035001 (2013), arXiv:1305.1108 [hep-ph].
- [186] Andrea Addazi, “Limiting First Order Phase Transitions in Dark Gauge Sectors from Gravitational Waves experiments,” *Mod. Phys. Lett.* **A32**, 1750049 (2017), arXiv:1607.08057 [hep-ph].
- [187] Thomas Hambye and Alessandro Strumia, “Dynamical generation of the weak and Dark Matter scale,” *Phys. Rev.* **D88**, 055022 (2013), arXiv:1306.2329 [hep-ph].
- [188] Michael J. Baker and Joachim Kopp, “Dark Matter Decay between Phase Transitions at the Weak Scale,” *Phys. Rev. Lett.* **119**, 061801 (2017), arXiv:1608.07578 [hep-ph].
- [189] Mayumi Aoki, Hiromitsu Goto, and Jisuke Kubo, “Gravitational Waves from Hidden QCD Phase Transition,” *Phys. Rev.* **D96**, 075045 (2017), arXiv:1709.07572 [hep-ph].
- [190] Andrea Addazi and Antonino Marciano, “Gravitational waves from dark first order phase transitions and dark photons,” *Chin. Phys.* **C42**, 023107 (2018), arXiv:1703.03248 [hep-ph].

- [191] Koji Tsumura, Masatoshi Yamada, and Yuya Yamaguchi, “Gravitational wave from dark sector with dark pion,” *JCAP* **1707**, 044 (2017), arXiv:1704.00219 [hep-ph].
- [192] Iason Baldes, “Gravitational waves from the asymmetric-dark-matter generating phase transition,” *JCAP* **1705**, 028 (2017), arXiv:1702.02117 [hep-ph].
- [193] Michael J. Baker, Moritz Breitbach, Joachim Kopp, and Lukas Mittnacht, “Dynamic Freeze-In: Impact of Thermal Masses and Cosmological Phase Transitions on Dark Matter Production,” *JHEP* **03**, 114 (2018), arXiv:1712.03962 [hep-ph].
- [194] Ligong Bian and Xuewen Liu, “Two-step strongly first-order electroweak phase transition modified FIMP dark matter, gravitational wave signals, and the neutrino mass,” *Phys. Rev.* **D99**, 055003 (2019), arXiv:1811.03279 [hep-ph].
- [195] Moritz Breitbach, Joachim Kopp, Eric Madge, Toby Opferkuch, and Pedro Schwaller, “Dark, Cold, and Noisy: Constraining Secluded Hidden Sectors with Gravitational Waves,” *JCAP* **1907**, 007 (2019), arXiv:1811.11175 [hep-ph].
- [196] Iason Baldes and Camilo Garcia-Cely, “Strong gravitational radiation from a simple dark matter model,” *JHEP* **05**, 190 (2019), arXiv:1809.01198 [hep-ph].
- [197] Djuna Croon, Verónica Sanz, and Graham White, “Model Discrimination in Gravitational Wave spectra from Dark Phase Transitions,” *JHEP* **08**, 203 (2018), arXiv:1806.02332 [hep-ph].
- [198] Eric Madge and Pedro Schwaller, “Leptophilic dark matter from gauged lepton number: Phenomenology and gravitational wave signatures,” *JHEP* **02**, 048 (2019), arXiv:1809.09110 [hep-ph].
- [199] Ligong Bian and Yi-Lei Tang, “Thermally modified sterile neutrino portal dark matter and gravitational waves from phase transition: The Freeze-in case,” *JHEP* **12**, 006 (2018), arXiv:1810.03172 [hep-ph].
- [200] Djuna Croon and Graham White, “Exotic Gravitational Wave Signatures from Simultaneous Phase Transitions,” *JHEP* **05**, 210 (2018), arXiv:1803.05438 [hep-ph].
- [201] Eleanor Hall, Thomas Konstandin, Robert McGehee, and Hitoshi Murayama, “Asymmetric Matters from a Dark First-Order Phase Transition,” (2019), arXiv:1911.12342 [hep-ph].
- [202] Malcolm Fairbairn, Edward Hardy, and Alastair Wickens, “Hearing without seeing: gravitational waves from hot and cold hidden sectors,” *JHEP* **07**, 044 (2019), arXiv:1901.11038 [hep-ph].
- [203] Andrey Katz and Antonio Riotto, “Baryogenesis and Gravitational Waves from Runaway Bubble Collisions,” *JCAP* **1611**, 011 (2016), arXiv:1608.00583 [hep-ph].
- [204] Andrew J. Long, Andrea Tesi, and Lian-Tao Wang, “Baryogenesis at a Lepton-Number-Breaking Phase Transition,” *JHEP* **10**, 095 (2017), arXiv:1703.04902 [hep-ph].
- [205] Paul Archer-Smith, Dylan Linthorne, and Daniel Stolarski, “Gravitational Wave Signals from Multiple Hidden Sectors,” *Phys. Rev.* **D101**, 095016 (2020), arXiv:1910.02083 [hep-ph].
- [206] Admir Greljo, Toby Opferkuch, and Ben A. Stefanek, “Gravitational Imprints of Flavor Hierarchies,” *Phys. Rev. Lett.* **124**, 171802 (2020), arXiv:1910.02014 [hep-ph].
- [207] Alexander J. Helmboldt, Jisuke Kubo, and Susan van der Woude, “Observational prospects for gravitational waves from hidden or dark chiral phase transitions,” *Phys. Rev.* **D100**, 055025 (2019), arXiv:1904.07891 [hep-ph].
- [208] Pedro Schwaller, “Gravitational Waves from a Dark Phase Transition,” *Phys. Rev. Lett.* **115**, 181101 (2015), arXiv:1504.07263 [hep-ph].
- [209] Claudio Corianò, Paul H. Frampton, and Alessandro Tatum, “Conformal unification in a quiver theory and gravitational waves,” *Phys. Lett.* **B811**, 135909 (2020), arXiv:2005.12216 [hep-ph].
- [210] Wei-Chih Huang, Francesco Sannino, and Zhi-Wei Wang, “Gravitational Waves from Pati-Salam Dynamics,” *Phys. Rev.* **D102**, 095025 (2020), arXiv:2004.02332 [hep-ph].
- [211] Nathaniel Craig, Noam Levi, Alberto Mariotti, and Diego Redigolo, “Ripples in Spacetime from Broken Supersymmetry,” *JHEP* **21**, 184 (2020), arXiv:2011.13949 [hep-ph].
- [212] Wei Chao, Wen-Feng Cui, Huai-Ke Guo, and Jing Shu, “Gravitational wave imprint of new symmetry breaking,” *Chin. Phys.* **C44**, 123102 (2020), arXiv:1707.09759 [hep-ph].
- [213] Fa Peng Huang and Xinmin Zhang, “Probing the gauge symmetry breaking of the early universe in 3-3-1 models and beyond by gravitational waves,” *Phys. Lett.* **B788**, 288–294 (2019), arXiv:1701.04338 [hep-ph].
- [214] Andrea Addazi, Yi-Fu Cai, and Antonino Marciano, “Testing Dark Matter Models with Radio Telescopes in light of Gravitational Wave Astronomy,” *Phys. Lett.* **B782**, 732–736 (2018), arXiv:1712.03798 [hep-ph].
- [215] Andrea Addazi and Antonino Marciano, “Limiting majoron self-interactions from gravitational wave experiments,” *Chin. Phys.* **C42**, 023105 (2018), arXiv:1705.08346 [hep-ph].
- [216] Venkitesh Ayyar, Thomas DeGrand, Daniel C. Hackett, William I. Jay, Ethan T. Neil, Yigal Shamir, and Benjamin Svetitsky, “Finite-temperature phase structure of SU(4) gauge theory with multiple fermion representations,” *Phys. Rev.* **D97**, 114502 (2018), arXiv:1802.09644 [hep-lat].
- [217] Nobuchika Okada and Osamu Seto, “Probing the seesaw scale with gravitational waves,” *Phys. Rev.* **D98**, 063532 (2018), arXiv:1807.00336 [hep-ph].
- [218] Katsuya Hashino, Mitsuru Kakizaki, Shinya Kanemura, Pyungwon Ko, and Toshinori Matsui, “Gravitational waves from first order electroweak phase transition in models with the U(1)<sub>X</sub> gauge symmetry,” *JHEP* **06**, 088 (2018), arXiv:1802.02947 [hep-ph].
- [219] Taiki Hasegawa, Nobuchika Okada, and Osamu Seto, “Gravitational waves from the minimal gauged U(1)<sub>B-L</sub> model,” *Phys. Rev.* **D99**, 095039 (2019), arXiv:1904.03020 [hep-ph].
- [220] Eleanor Hall, Thomas Konstandin, Robert McGehee, Hitoshi Murayama, and Géraldine Servant, “Baryogenesis From a Dark First-Order Phase Transition,” *JHEP* **04**, 042 (2020), arXiv:1910.08068 [hep-ph].
- [221] Aleksandr Azatov, Daniele Barducci, and Francesco Sgarlata, “Gravitational traces of broken gauge symmetries,” *JCAP* **2007**, 027 (2020), arXiv:1910.01124 [hep-ph].
- [222] Naoyuki Haba and Toshifumi Yamada, “Gravitational waves from phase transition in minimal SUSY

- $U(1)_{B-L}$  model,” *Phys. Rev.* **D101**, 075027 (2020), arXiv:1911.01292 [hep-ph].
- [223] Tathagata Ghosh, Huai-Ke Guo, Tao Han, and Hongkai Liu, “Electroweak phase transition with an  $SU(2)$  dark sector,” *JHEP* **07**, 045 (2021), arXiv:2012.09758 [hep-ph].
- [224] Nobuchika Okada, Osamu Seto, and Hikaru Uchida, “Gravitational waves from breaking of an extra  $U(1)$  in  $SO(10)$  grand unification,” *PTEP* **2021**, 033B01 (2021), arXiv:2006.01406 [hep-ph].
- [225] James Halverson, Cody Long, Anindita Maiti, Brent Nelson, and Gustavo Salinas, “Gravitational waves from dark Yang-Mills sectors,” *JHEP* **05**, 154 (2021), arXiv:2012.04071 [hep-ph].
- [226] P. S. Bhupal Dev and A. Mazumdar, “Probing the Scale of New Physics by Advanced LIGO/VIRGO,” *Phys. Rev.* **D93**, 104001 (2016), arXiv:1602.04203 [hep-ph].
- [227] Luigi Delle Rose, Giuliano Panico, Michele Redi, and Andrea Tesi, “Gravitational Waves from Supercool Axions,” *JHEP* **04**, 025 (2020), arXiv:1912.06139 [hep-ph].
- [228] Benedict Von Harling, Alex Pomarol, Oriol Pujolàs, and Fabrizio Rompineve, “Peccei-Quinn Phase Transition at LIGO,” *JHEP* **04**, 195 (2020), arXiv:1912.07587 [hep-ph].
- [229] Djuna Croon, Rachel Houtz, and Verónica Sanz, “Dynamical Axions and Gravitational Waves,” *JHEP* **07**, 146 (2019), arXiv:1904.10967 [hep-ph].
- [230] P. S. Bhupal Dev, Francesc Ferrer, Yiyang Zhang, and Yongchao Zhang, “Gravitational Waves from First-Order Phase Transition in a Simple Axion-Like Particle Model,” *JCAP* **1911**, 006 (2019), arXiv:1905.00891 [hep-ph].
- [231] Camila S. Machado, Wolfram Ratzinger, Pedro Schwaller, and Ben A. Stefanek, “Gravitational wave probes of axionlike particles,” *Phys. Rev.* **D102**, 075033 (2020), arXiv:1912.01007 [hep-ph].
- [232] Cheng-Wei Chiang and Bo-Qiang Lu, “Testing clockwork axion with gravitational waves,” *JCAP* **05**, 049 (2021), arXiv:2012.14071 [hep-ph].
- [233] Anish Ghoshal and Alberto Salvio, “Gravitational waves from fundamental axion dynamics,” *JHEP* **12**, 049 (2020), arXiv:2007.00005 [hep-ph].
- [234] Tillmann Boeckel and Jurgen Schaffner-Bielich, “A little inflation in the early universe at the QCD phase transition,” *Phys. Rev. Lett.* **105**, 041301 (2010), [Erratum: *Phys. Rev. Lett.* 106,069901(2011)], arXiv:0906.4520 [astro-ph.CO].
- [235] Simon Schettler, Tillmann Boeckel, and Jurgen Schaffner-Bielich, “Imprints of the QCD Phase Transition on the Spectrum of Gravitational Waves,” *Phys. Rev.* **D83**, 064030 (2011), arXiv:1010.4857 [astro-ph.CO].
- [236] Tillmann Boeckel and Jurgen Schaffner-Bielich, “A little inflation at the cosmological QCD phase transition,” *Phys. Rev.* **D85**, 103506 (2012), arXiv:1105.0832 [astro-ph.CO].
- [237] Salvatore Capozziello, Mohsen Khodadi, and Gaetano Lambiase, “The quark chemical potential of QCD phase transition and the stochastic background of gravitational waves,” *Phys. Lett.* **B789**, 626–633 (2019), arXiv:1808.06188 [gr-qc].
- [238] Mohsen Khodadi, Kouros Nozari, Habib Abedi, and Salvatore Capozziello, “Planck scale effects on the stochastic gravitational wave background generated from cosmological hadronization transition: A qualitative study,” *Phys. Lett.* **B783**, 326–333 (2018), arXiv:1805.11310 [gr-qc].
- [239] Yang Bai and Andrew J. Long, “Six Flavor Quark Matter,” *JHEP* **06**, 072 (2018), arXiv:1804.10249 [hep-ph].
- [240] Francesco Bigazzi, Alessio Caddeo, Aldo L. Cotrone, and Angel Paredes, “Dark Holograms and Gravitational Waves,” *JHEP* **04**, 094 (2021), arXiv:2011.08757 [hep-ph].
- [241] Wei-Chih Huang, Manuel Reichert, Francesco Sannino, and Zhi-Wei Wang, “Testing the dark  $SU(N)$  Yang-Mills theory confined landscape: From the lattice to gravitational waves,” *Phys. Rev. D* **104**, 035005 (2021), arXiv:2012.11614 [hep-ph].
- [242] Manuel Reichert, Francesco Sannino, Zhi-Wei Wang, and Chen Zhang, “Dark confinement and chiral phase transitions: gravitational waves vs matter representations,” *JHEP* **01**, 003 (2022), arXiv:2109.11552 [hep-ph].
- [243] Iason Baldes and Géraldine Servant, “High scale electroweak phase transition: baryogenesis & symmetry non-restoration,” *JHEP* **10**, 053 (2018), arXiv:1807.08770 [hep-ph].
- [244] Alfredo Glioti, Riccardo Rattazzi, and Luca Vecchi, “Electroweak Baryogenesis above the Electroweak Scale,” *JHEP* **04**, 027 (2019), arXiv:1811.11740 [hep-ph].
- [245] Patrick Meade and Harikrishnan Ramani, “Unrestored Electroweak Symmetry,” *Phys. Rev. Lett.* **122**, 041802 (2019), arXiv:1807.07578 [hep-ph].
- [246] Oleksii Matsedonskyi and Geraldine Servant, “High-Temperature Electroweak Symmetry Non-Restoration from New Fermions and Implications for Baryogenesis,” *JHEP* **09**, 012 (2020), arXiv:2002.05174 [hep-ph].
- [247] Qing-Hong Cao, Katsuya Hashino, Xu-Xiang Li, Zhe Ren, and Jiang-Hao Yu, “Electroweak phase transition triggered by fermion sector,” *JHEP* **01**, 001 (2022), arXiv:2103.05688 [hep-ph].
- [248] Marieke Postma and Graham White, “Cosmological phase transitions: is effective field theory just a toy?” *JHEP* **03**, 280 (2021), arXiv:2012.03953 [hep-ph].
- [249] José Eliel Camargo-Molina, Rikard Enberg, and Johan Löfgren, “A new perspective on the electroweak phase transition in the Standard Model Effective Field Theory,” *JHEP* **10**, 127 (2021), arXiv:2103.14022 [hep-ph].
- [250] Oliver Gould, Jonathan Kozaczuk, Lauri Niemi, Michael J. Ramsey-Musolf, Tuomas V. I. Tenkanen, and David J. Weir, “Nonperturbative analysis of the gravitational waves from a first-order electroweak phase transition,” *Phys. Rev. D* **100**, 115024 (2019), arXiv:1903.11604 [hep-ph].
- [251] Kimmo Kainulainen, Venus Keus, Lauri Niemi, Kari Rummukainen, Tuomas V. I. Tenkanen, and Ville Vaskonen, “On the validity of perturbative studies of the electroweak phase transition in the Two Higgs Doublet model,” *JHEP* **06**, 075 (2019), arXiv:1904.01329 [hep-ph].
- [252] Lauri Niemi, Philipp Schicho, and Tuomas V. I. Tenkanen, “Singlet-assisted electroweak phase transition at two loops,” *Phys. Rev. D* **103**, 115035 (2021), arXiv:2103.07467 [hep-ph].
- [253] Djuna Croon, Oliver Gould, Philipp Schicho, Tuomas V. I. Tenkanen, and Graham White, “Theoretical uncertainties for cosmological first-order phase transi-

- tions,” *JHEP* **04**, 055 (2021), arXiv:2009.10080 [hep-ph].
- [254] Oliver Gould and Tuomas V. I. Tenkanen, “On the perturbative expansion at high temperature and implications for cosmological phase transitions,” *JHEP* **06**, 069 (2021), arXiv:2104.04399 [hep-ph].
- [255] Oliver Gould and Joonas Hirvonen, “Effective field theory approach to thermal bubble nucleation,” *Phys. Rev. D* **104**, 096015 (2021), arXiv:2108.04377 [hep-ph].
- [256] Johan Löfgren, Michael J. Ramsey-Musolf, Philipp Schicho, and Tuomas V. I. Tenkanen, “Nucleation at finite temperature: a gauge-invariant, perturbative framework,” (2021), arXiv:2112.05472 [hep-ph].
- [257] Joonas Hirvonen, Johan Löfgren, Michael J. Ramsey-Musolf, Philipp Schicho, and Tuomas V. I. Tenkanen, “Computing the gauge-invariant bubble nucleation rate in finite temperature effective field theory,” (2021), arXiv:2112.08912 [hep-ph].
- [258] Sidney R. Coleman and Erick J. Weinberg, “Radiative Corrections as the Origin of Spontaneous Symmetry Breaking,” *Phys. Rev. D* **7**, 1888–1910 (1973).
- [259] Eldad Gildener and Steven Weinberg, “Symmetry Breaking and Scalar Bosons,” *Phys. Rev. D* **13**, 3333 (1976).
- [260] Kazuhiro Endo and Yukinari Sumino, “A Scale-invariant Higgs Sector and Structure of the Vacuum,” *JHEP* **05**, 030 (2015), arXiv:1503.02819 [hep-ph].
- [261] Katy Hally, Heather E. Logan, and Terry Pilkington, “Constraints on large scalar multiplets from perturbative unitarity,” *Phys. Rev. D* **85**, 095017 (2012), arXiv:1202.5073 [hep-ph].
- [262] Kevin Earl, Katy Hartling, Heather E. Logan, and Terry Pilkington, “Constraining models with a large scalar multiplet,” *Phys. Rev. D* **88**, 015002 (2013), arXiv:1303.1244 [hep-ph].
- [263] Georges Aad et al. (ATLAS), “Combined measurements of Higgs boson production and decay using up to 80 fb<sup>-1</sup> of proton-proton collision data at  $\sqrt{s} = 13$  TeV collected with the ATLAS experiment,” *Phys. Rev. D* **101**, 012002 (2020), arXiv:1909.02845 [hep-ex].
- [264] Brian Henning, Xiaochuan Lu, and Hitoshi Murayama, “How to use the Standard Model effective field theory,” *JHEP* **01**, 023 (2016), arXiv:1412.1837 [hep-ph].
- [265] L. Dolan and R. Jackiw, “Symmetry Behavior at Finite Temperature,” *Phys. Rev. D* **9**, 3320–3341 (1974).
- [266] M. E. Carrington, “The Effective potential at finite temperature in the Standard Model,” *Phys. Rev. D* **45**, 2933–2944 (1992).
- [267] Katsuya Hashino, Shinya Kanemura, and Yuta Orikasa, “Discriminative phenomenological features of scale invariant models for electroweak symmetry breaking,” *Phys. Lett. B* **752**, 217–220 (2016), arXiv:1508.03245 [hep-ph].
- [268] Sidney R. Coleman, “The Fate of the False Vacuum. 1. Semiclassical Theory,” *Phys. Rev. D* **15**, 2929–2936 (1977), [Erratum: *Phys. Rev. D* **16**, 1248(1977)].
- [269] Curtis G. Callan, Jr. and Sidney R. Coleman, “The Fate of the False Vacuum. 2. First Quantum Corrections,” *Phys. Rev. D* **16**, 1762–1768 (1977).
- [270] Andrei D. Linde, “Fate of the False Vacuum at Finite Temperature: Theory and Applications,” *Phys. Lett.* **100B**, 37–40 (1981).
- [271] Andrei D. Linde, “Decay of the False Vacuum at Finite Temperature,” *Nucl. Phys.* **B216**, 421 (1983), [Erratum: *Nucl. Phys.* **B223**, 544(1983)].
- [272] Alan H. Guth and Erick J. Weinberg, “Could the Universe Have Recovered from a Slow First Order Phase Transition?” *Nucl. Phys. B* **212**, 321–364 (1983).
- [273] Michael S. Turner, Erick J. Weinberg, and Lawrence M. Widrow, “Bubble nucleation in first order inflation and other cosmological phase transitions,” *Phys. Rev. D* **46**, 2384–2403 (1992).
- [274] John Ellis, Marek Lewicki, and José Miguel No, “On the Maximal Strength of a First-Order Electroweak Phase Transition and its Gravitational Wave Signal,” *JCAP* **04**, 003 (2019), arXiv:1809.08242 [hep-ph].
- [275] John Ellis, Marek Lewicki, and José Miguel No, “Gravitational waves from first-order cosmological phase transitions: lifetime of the sound wave source,” *JCAP* **2007**, 050 (2020), arXiv:2003.07360 [hep-ph].
- [276] Xiao Wang, Fa Peng Huang, and Xinmin Zhang, “Phase transition dynamics and gravitational wave spectra of strong first-order phase transition in supercooled universe,” *JCAP* **2005**, 045 (2020), arXiv:2003.08892 [hep-ph].
- [277] Arthur Kosowsky, Michael S. Turner, and Richard Watkins, “Gravitational radiation from colliding vacuum bubbles,” *Phys. Rev. D* **45**, 4514–4535 (1992).
- [278] Arthur Kosowsky, Michael S. Turner, and Richard Watkins, “Gravitational waves from first order cosmological phase transitions,” *Phys. Rev. Lett.* **69**, 2026–2029 (1992).
- [279] Arthur Kosowsky and Michael S. Turner, “Gravitational radiation from colliding vacuum bubbles: envelope approximation to many bubble collisions,” *Phys. Rev. D* **47**, 4372–4391 (1993), arXiv:astro-ph/9211004 [astro-ph].
- [280] Marc Kamionkowski, Arthur Kosowsky, and Michael S. Turner, “Gravitational radiation from first order phase transitions,” *Phys. Rev. D* **49**, 2837–2851 (1994), arXiv:astro-ph/9310044 [astro-ph].
- [281] Stephan J. Huber and Thomas Konstandin, “Gravitational Wave Production by Collisions: More Bubbles,” *JCAP* **0809**, 022 (2008), arXiv:0806.1828 [hep-ph].
- [282] Mark Hindmarsh, Stephan J. Huber, Kari Rummukainen, and David J. Weir, “Gravitational waves from the sound of a first order phase transition,” *Phys. Rev. Lett.* **112**, 041301 (2014), arXiv:1304.2433 [hep-ph].
- [283] Mark Hindmarsh, Stephan J. Huber, Kari Rummukainen, and David J. Weir, “Numerical simulations of acoustically generated gravitational waves at a first order phase transition,” *Phys. Rev. D* **92**, 123009 (2015), arXiv:1504.03291 [astro-ph.CO].
- [284] Mark Hindmarsh, Stephan J. Huber, Kari Rummukainen, and David J. Weir, “Shape of the acoustic gravitational wave power spectrum from a first order phase transition,” *Phys. Rev. D* **96**, 103520 (2017), [erratum: *Phys. Rev. D* **101**, no.8, 089902(2020)], arXiv:1704.05871 [astro-ph.CO].
- [285] Daniel Cutting, Mark Hindmarsh, and David J. Weir, “Vorticity, kinetic energy, and suppressed gravitational wave production in strong first order phase transitions,” *Phys. Rev. Lett.* **125**, 021302 (2020), arXiv:1906.00480 [hep-ph].
- [286] Huai-Ke Guo, Kuver Sinha, Daniel Vagie, and Graham White, “Phase Transitions in an Expanding Universe: Stochastic Gravitational Waves in Standard

- and Non-Standard Histories,” JCAP **01**, 001 (2021), arXiv:2007.08537 [hep-ph].
- [287] Jose R. Espinosa, Thomas Konstandin, Jose M. No, and Geraldine Servant, “Energy Budget of Cosmological First-order Phase Transitions,” JCAP **1006**, 028 (2010), arXiv:1004.4187 [hep-ph].
- [288] Tyler Corbett, Aniket Joglekar, Hao-Lin Li, and Jiang-Hao Yu, “Exploring Extended Scalar Sectors with Di-Higgs Signals: A Higgs EFT Perspective,” JHEP **05**, 061 (2018), arXiv:1705.02551 [hep-ph].
- [289] Hao-Lin Li, Zhe Ren, Jing Shu, Ming-Lei Xiao, Jiang-Hao Yu, and Yu-Hui Zheng, “Complete set of dimension-eight operators in the standard model effective field theory,” Phys. Rev. D **104**, 015026 (2021), arXiv:2005.00008 [hep-ph].
- [290] Hao-Lin Li, Zhe Ren, Ming-Lei Xiao, Jiang-Hao Yu, and Yu-Hui Zheng, “Complete set of dimension-nine operators in the standard model effective field theory,” Phys. Rev. D **104**, 015025 (2021), arXiv:2007.07899 [hep-ph].
- [291] Christopher T. Hill, “Is the Higgs Boson Associated with Coleman-Weinberg Dynamical Symmetry Breaking?” Phys. Rev. D **89**, 073003 (2014), arXiv:1401.4185 [hep-ph].
- [292] Alexander J. Helmboldt, Pascal Humbert, Manfred Lindner, and Juri Smirnov, “Minimal conformal extensions of the Higgs sector,” JHEP **07**, 113 (2017), arXiv:1603.03603 [hep-ph].
- [293] Pankaj Agrawal, Debashis Saha, Ling-Xiao Xu, Jiang-Hao Yu, and C. P. Yuan, “Determining the shape of the Higgs potential at future colliders,” Phys. Rev. D **101**, 075023 (2020), arXiv:1907.02078 [hep-ph].